TRIBHUVAN UNIVERSITY
INSTITUTE OF ENGINEERING
PULCHOWK CAMPUS

Thesis No:M-85-MSMDE-2021-2024

Experimental Analysis of Fluid Flow and Heat Transfer of Al_2O_3-Water Nanofluid in Turbulated Tube

by

Sudeep Sah

A THESIS
REPORT SUBMITTED TO THE DEPARTMENT OF MECHANICAL AND AEROSPACE ENGINEERING IN PARTIAL FULFILLMENT OF THE REQUIREMENTS FOR THE DEGREE OF MASTER OF SCIENCE IN MECHANICAL SYSTEM DESIGN AND ENGINEERING

DEPARTMENT OF MECHANICAL AND AEROSPACE ENGINEERING
LALITPUR,NEPAL

JUNE 2024

COPYRIGHT

TRIBHUVAN UNIVERSITY

INSTITUTE OF ENGINEERING

PULCHOWK CAMPUS

DEPARTMENT OF MECHANICAL AND AEROSPACE ENGINEERING

The undersigned certify that they have read, and recommended to the Institute of Engineering for acceptance, a thesis entitled **"Experimental Analysis of Fluid Flow and Heat Transfer of Al_2O_3-Water Nanofluid in Turbulated Tube".** submitted by Sudeep Sah for the Final Thesis Report in partial fulfillment of the requirements for the degree of Master of Science in Mechanical System Design and Engineering.

....

Supervisor, Surya Pd. Adhikari, PhD

Associate Professor

Department of Mechanical and Aerospace Engineering

....

External Examiner, Ranjit Shrestha, PhD

Assistant Professor

Department of Mechanical Engineering

Kathmandu University

Tribhuvan University
Institute of Engineering
Department of Mechanical and Aerospace Engineering
Pulchowk Campus

....

Committee Chairperson, Sudip Bhattrai, PhD

Assistant Professor/ Head of the Department

Department of Mechanical and Aerospace Engineering

Date: 9th June, 2024

2

ABSTRACT

Nanofluids have garnered significant interest because of their enhanced thermal properties. One prominent application of nanofluids is enhancing the thermal performance of heat exchangers. In this research work, experimental investigations were conducted to evaluate the effect of adding Al_2O_3-water nanofluids on the overall heat transfer coefficient and pressure drop in a shell and tube heat exchanger fitted with helical coil turbulators. Al_2O_3 nanoparticles were uniformly dispersed in water to create nanofluids with concentrations of 0.2% and 0.4% by weight. These nanofluids were used in tube of the heat exchanger, where helical coil turbulators with pitches of 16mm and 20mm induced turbulence to enhance heat transfer. The study examined various parameters including nanofluid concentration and turbulator pitch, analyzing their effects on pressure drop and heat transfer.

The study presents the outcomes indicating that the use of Al_2O_3-water nanofluids leads to a significant enhancement of thermal efficiency of shell and tube heat exchanger. The maximum increase in overall heat transfer coefficient was observed with the 0.4% Al_2O_3-Water nanofluid combined with a 16mm pitch helical coil. Furthermore, employing the 16mm pitch coil resulted in a higher pressure drop compared to the 20mm pitch coil, highlighting the trade-off between heat transfer enhancement and pressure drop.

The average enhancements in the overall heat transfer coefficient for the 0.2% and 0.4% nanofluids without turbulators were 19.5% and 34.66%, respectively, within the flow rate range of 470 to 620 l/hr compared to pure water. Introducing 16mm and 20mm helical coil turbulators in pure water increased the overall heat transfer coefficient by 47.09% to 54.76% and 26.7% to 34.66%, respectively, relative to pure water without turbulator.

ACKNOWLEDGMENTS

I would like to express my sincere gratitude to Associate Professor Surya Prasad Adhikari, PhD for supervising my thesis work. Without his invaluable advice, this research work would not been concluded.

I would also like to thank Mr. Anil Muni Bajracharya, Principal of Shankaharapur Polytechnical Institute, Ctevt for allowing me to use the Workshop facilities for my research. Furthermore I would also like to thank Er. Roshan Kumar Thakur and Er. Abhishek Karki of Shankharapur Polytechnic Institute for continuously helping with fabrication and experimental works.

I am also very thankful to Er. Shah Nawaj Ansari and Mr. Sahil Sharma of Nepal Academy for Science and Technology(NAST) for helping me to prepare nanofluid.

I want to express my gratitude to everyone who has assisted me in this thesis work in different ways.

TABLE OF CONTENTS

List of Figures

LIST OF TABLES

LIST OF SYMBOLS

A : total heat transfer area(m^2)

Cp : specific heat capacity of the fluid (kJ/kgK)

D : characteristic length scale of the system (m)

f : external force acting on the fluid(N)

h : convective heat transfer coefficient (W/m^2K)

k : thermal conductivity of the fluid (W/m^2K)

k_{nf} : thermal conductivity of nanofluids (W/m^2K)

k_{np} : thermal conductivity of nanoparticles (W/m^2K)

k_{bf} : thermal conductivity of base fluid (W/m^2K)

L : characteristic length scale (m)

Nu : Nusselt Number

p : pressure (Pa)

Q : Heat transfer (W)

Re : Reynold Number

t : time (s)

T : temperature (K)

T_{h1} : inlet temperatures of hot stream (K)

T_{h2} : outlet temperatures of hot stream (K)

T_{C1} : inlet temperatures of cold stream (K)

T_{C2} : outlet temperatures of cold stream(K)

u : velocity (m^2/s)

U : Overall heat transfer cooeffiecient (W/m2K)

v : velocity of the flow (m^2/s)

V : Flow rate (m^3/s)

ρ : density of the fluid (kg/m^3)

ρ_{nf} : nanofluid density (kg/m^3)

ρ_{np} : nanoparticle density(kg/m^3)

ρ_{bf} : base fluid density(kg/m^3)

μ : dynamic viscosity of the fluid

ϕ : fraction of nanoparticles

CHAPTER ONE: INTRODUCTION

1.1 Background

Heat exchangers are widely used in various industries to facilitate heat transfer between different fluids, with the goal of recovering waste heat and reducing utility costs (M. Fares et al., 2020). Nanofluids have gained considerable attention over the past few decades because of their improved thermal properties and flow characteristics (Das et al., 2006). These characteristics enable nanofluids to improve heat transfer efficiency in heat exchangers.

Numerous experimental studies have investigated the heat transfer characteristics of nanofluids in various types of heat exchangers. For instance, Shahrul et al. (2014) conducted analytical study on a shell and tube heat exchanger utilizing nanofluids containing Fe_3O_4, ZnO, TiO_2, CuO, and Al_2O_3 nanoparticles. Their findings highlighted that the highest heat transfer coefficient was of Al_2O_3-water among the tested nanofluids.

Various techniques have been used to improve heat transfer, including magnetic fields, geometric modifications, ribs and baffles, surface roughness, and the incorporation of nanoparticles. Nanofluids, in particular, have shown significant potential as a new class of fluids with superior thermal performance (T. Salameh et al., 2023). Research indicates that using nanofluids instead of conventional base fluids enhances heat transfer, as demonstrated through experiments and simulations in concentric counter-flow tube heat exchangers.

Nanofluids are known for their ability to improve thermal conductivity. Additionally, turbulent flow within tubes further enhances heat transfer efficiency. Therefore, combining nanofluids with turbulent flow in tubes has the ability to substantially increase heat transfer rates.

The unique properties of nanofluids, including enhanced thermal conductivity, specific heat capacity, and convective heat transfer coefficient, make them suitable for a different heat transfer applications. The heat transfer and flow characteristics of nanofluids are influenced by various factors, such as nanoparticle shape, size, concentration, surface properties, flow conditions and base fluid properties.

Experimental studies have demonstrated that increasing concentration of nanoparticle significantly enhance the convective heat transfer coefficient and thermal conductivity of nanofluids. Nonetheless, higher nanoparticle concentrations also lead to increased pressure drop and viscosity, which can result in higher pumping costs and reduced flow rates (Shabi et al., 2024).

Various theoretical and numerical modeling studies have been carried out to predict the heat transfer and flow behavior of nanofluids. These efforts aim to create accurate models for predicting the convective heat transfer coefficient, flow characteristics, thermal conductivity and overall heat transfer performance of nanofluids in various configuration.

1.2 Problem Statement

Efficient heat exchangers are crucial for optimizing performance and achieving energy savings in diverse industrial processes. Conventional heat transfer fluids like ethylene glycol, oil and water often struggle to meet the required thermal performance standards, particularly in high-demand applications. In recent decades, Nanofluids have become a better solution for enhancing heat transfer rates due to their superior thermal properties.

Despite extensive research highlighting the nanofluids potential, the combined impact of concentration of nanoparticle, fluid flow dynamics, and turbulence inducing structures on pressure drop and heat transfer efficiency remains inadequately understood. Specifically, there is a notable gap in comprehensive experimental and numerical data concerning the Al_2O_3-water nanofluids performance in shell and tube heat exchangers equipped with helical coil turbulators. These turbulators enhance heat transfer by inducing turbulence but also contribute to increased pressure drops, presenting a critical trade-off that must be optimized for practical applications.

Therefore, the primary objective is to investigate how varying concentrations of Al_2O_3 nanoparticles and the use of helical coil turbulators with different pitches influence the overall heat transfer coefficient and also pressure drop in shell and tube heat exchangers. Additionally, comparative analyses involving pure water and nanofluids without turbulators are essential to isolate and quantify the benefits and drawbacks of these enhancements. This research aims to provide deeper insights into these factors to facilitate the design and optimization of more efficient heat exchange system.

1.3 Objectives

1.3.1 Main Objectives

The primary objective of this research is to investigate the fluid flow and heat transfer characteristics of Al_2O_3-Water nanofluids in turbulated tubes.

1.3.2 Specific Objectives

The specific objectives are:

- To Synthesize Al_2O_3 nanoparticle.
- To Blend nanoparticle at different concentration to the base fluid.
- To measure the overall heat transfer coefficient and pressure drop of Al_2O_3-Water nanofluids in different turbulated tubes experimentally.
- To investigate the effect of nanoparticle concentration and flow rate on the overall heat transfer coefficient and pressure drop of nanofluids in turbulated tubes.

1.4 Limitations of Research

The study may be intervened by different difficulties and limitations. Some of the limitations are listed below.

- Specific Nanoparticle Type and Concentrations: The study focuses exclusively on Al_2O_3 nanoparticles at concentrations of 0.2% and 0.4% by weight. The applicability of these findings to other types of nanoparticles or different concentration levels, limiting the generalizability of the results.

- Experimental Conditions: The experiments were conducted under specific flow rates (470 to 620 l/hr) and temperature conditions. Variations in these parameters might influence the overall heat transfer coefficient and pressure drop differently, which was not explored in this study.

- Helical Coil Turbulator Pitches: Only two turbulator pitches (16mm and 20mm) were examined. Other geometrical configurations and pitch variations might yield different results, and their impacts on thermal performance and pressure drop were not considered.

- Long-term Stability and Fouling: The long-term stability of the Aluminium Oxide (Al_2O_3) nanoparticles in water and potential fouling effects on the heat exchanger surfaces were not addressed. These factors could significantly impact the practical application and maintenance requirements of Al2O3-water nanofluid based heat exchangers.

- Numerical Simulation Constraints: The numerical simulations employed certain assumptions and simplifications to model the flow and heat transfer characteristics. These assumptions might not fully capture the complexities of real-world applications, potentially affecting the accuracy of the predictions.

- Environmental Considerations: The study did not explore the environmental impact of using Al_2O_3-water nanofluids in industrial heat exchangers.

CHAPTER TWO: LITERATURE REVIEW

2.1 Turbulent Flow and Heat Transfer

Turbulent flow has been extensively researched for its profound impact on enhancing heat transfer rates in fluids. It is widely acknowledged that turbulent flow can significantly augment heat transfer compared to laminar flow.

Akyurek et al. (2018) conducted experimental research using nanofluids in a concentric tube heat exchanger with wire coil turbulators. They observed that higher nanoparticle concentrations enhanced the total heat transfer coefficient. Furthermore, they found that elevated Reynolds numbers and the turbulent flow induced by the turbulators boosted heat transfer rates but pressure drop also increased across the heat exchanger.

Chandrasekhar et al. (2016) investigated friction factor and heat transfer in a horizontal tube in turbulent flow conditions. They noted that while turbulent flow enhances heat transfer rates, it also results in higher friction factors. This trade-off between improved heat transfer and increased flow resistance is an essential consideration in heat exchanger design.

Murugesan et al. (2017) studied turbulent flow in a circular tube equipped with twisted tape inserts. They found that both heat transfer rates and friction factors escalate by increasing Reynolds numbers. Their findings underscored that turbulent flow can substantially enhance heat transfer, particularly at higher Reynolds numbers, albeit at the cost of increased friction within the tube.

Kia et al. (2023) studied heat transfer and pressure drop in helical tubes using Al_2O_3 and SiO_2 nanofluids with base oil at different concentrations. Their findings revealed that Al_2O_3 nanofluids notably increase heat transfer coefficients, and helical tube geometries provide better heat transfer than straight tubes. Additionally, optimizing the pitch and diameter of tubes further improved overall performance.

Collectively, these studies highlight that turbulent flow can significantly enhance heat transfer rates in fluids. The extent of this enhancement depends on factors such as Reynolds number, flow channel geometry, and the presence of turbulence promoting devices. However, designers must carefully weigh the profits of enhanced heat transfer against the accompanying increases in pressure drop when optimizing heat transfer systems for industrial applications

2.2 Literature Survey

Many experimental studies have explored the flow and heat transfer characteristics of nanofluid in turbulated tube. A summary of relevant literature includes:

1. Shabi et al. (2024): Investigated heat transfer performance of Al2O3-water nanofluid by varying nanoparticle concentrations in shell and helical coiled heat exchanger. The study revealed that increasing nanofluid concentration enhanced both pressure drop and heat transfer coefficient.
2. T. Salameh et al. (2023): Combined experimental and numerical analyses to investigate heat transfer improvement in a concentric counter flow tube heat exchanger using different nanofluids. Their findings highlighted significant improvements in heat exchanger performance compared to base liquids.
3. Arun Kumar Tiwari, Pradyumna Ghosh, and Jahar Sarkar (2015): Investigated the influence of various nanoparticle concentration on the overall heat transfer coefficient in a plate heat exchanger. They founded that higher particle concentrations led to enhanced heat transfer rates.
4. Shahrul et al. (2014): Evaluated operational efficiency of shell and tube heat exchanger at various mass flow rates utilizing nanofluid . They found that when mass flow rate increases then heat transfer rates also increases.
5. Akyürek et al. (2018): Investigated the effects of concentration of nanoparticle in a concentric tube heat exchanger with wire coil turbulator. Their study demonstrated that increasing concentration of nanoparticle and Reynolds number improved heat transfer coefficient but also resulted in higher pressure drops. Notably, low-concentration nanofluids exhibited pressure drops similar to water, while the use of turbulators increased pressure drop further.
6. Suresh et al. (2012): Experimentally investigated pressure drop and heat transfer in circular tubes utilizing spiraled rod inserts and Al_2O_3-water nanofluids. Their findings indicated a notable enhancement in heat transfer due to nanoparticles, resulting in higher Nusselt numbers compared to plain tubes. However, the study also observed increased pressure drop with spiraled rod inserts compared to plain tubes.

These studies collectively underscore that nanofluids can significantly augment convective heat transfer coefficients, with turbulated tubes further enhancing this effect. These findings provide valuable insights for the heat exchangers design for improving efficiency and performance.

2.3 Shell and Tube Heat Exchanger and Helical coil Turbulator

A shell and tube heat exchanger is a widely used device in various industrial processes for transferring heat between two fluids. It comprises a series of tubes, with one set with the hot fluid and the other set with the cold fluid. This design facilitates efficient heat transfer without mixing the fluids. Shell and tube heat exchanger can accommodate a various range of fluids, including Al_2O_3-water nanofluids, making them versatile for experimental setups where different fluid properties and concentrations need to be tested. They are suitable for a broad range of temperatures and pressures, making them ideal for high-performance applications and diverse experimental conditions. The design inherently provides huge surface area for heat exchange between shell and tube sides, enhancing the overall heat transfer rate. Additionally, shell and tube heat exchangers are known for their mechanical strength and durability, essential for withstanding the operational stresses in experimental setups involving high flow rates and nanoparticle suspensions（Ramesh K. Shah and Dusan P. Sekulic, 2003）.

Turbulators are devices or inserts placed inside fluid flow channels to enhance heat transfer by promoting turbulence within the flow. They disrupt the laminar flow regime, increasing fluid mixing and enhancing the convective heat transfer coefficient. Turbulators are commonly used in heat exchangers and other thermal management systems to improve thermal performance. Helical coil turbulators, in particular, increases effective heat transfer area within tube, promoting better thermal contact between the the tube wall and the fluid. The helical coils create secondary flows and induce turbulence even at lower Reynolds numbers. This disturbance of the thermal boundary layer significantly enhances heat transfer coefficient（Jian Guo, Aiwu Fan, Xiaoyu Zhang and Wei Liu, 2011）.

These enhancements make helical coil turbulators a valuable addition to heat exchanger, improving their overall heat transfer rate and making them suitable for advanced applications in heat transfer research and industrial processes.

2.4 Nanoparticles and Nanofluids

Nanoparticles refer to particles sized between 1 and 100 nanometers, known for their unique properties such as large surface area to volume ratio and distinct surface properties. These characteristics make nanoparticles valuable across diverse fields including electronics, medicine, and energy.

Nanofluids are fluids comprising a base fluid (e.g., oil, ethylene glycol, water) with dispersed nanoparticles, which can be metallic or non-metallic. The addition of nanoparticles significantly improves the thermal properties of the base fluid. This enhancement stems from the nanoparticles' high surface area to volume ratio that boosts convective heat transfer coefficients and thermalconductivity.

Research has explored the use of nanofluids in enhancing the heat exchanger's thermal performance. For instance, Shahrul et al. (2014) explored the thermal conductivity in shell and tube heat exchanger utilizing nanofluids containing Fe_3O_4, ZnO, TiO_2, CuO and Al_2O_3 nanoparticles, highlighting the highest heat transfer coefficients was achieved for Al_2O_3-water nanofluids. Similarly, Albadr et al. (2013) investigated the convective heat transfer properties of Al_2O_3-water nanofluids across varying concentrations in a horizontal shell and tube heat exchanger, noting moderate improvements in heat transfer coefficient.

These studies underscore potential of nanofluids, particularly those incorporating Al_2O_3 nanoparticles, to improve the thermal efficiency of heat exchangers through improved heat transfer capabilities.

Nanoparticles introduced into a fluid can significantly alter its thermophysical properties. Some of these affected properties include:

- Thermal conductivity : Incorporating nanoparticles enhances the fluid's thermal conductivity due to the large surface area to volume ratio, facilitating more efficient thermal energy transfer between the fluid and its surroundings.
- Viscosity : The fluid's viscosity is increases with the addition of nanoparticle. This occurs as nanoparticles can agglomerate, creating clusters that impede fluid flow.
- Specific heat : Nanoparticles increase fluid's specific heat by virtue of their higher heat capacity compared to the base fluid.

- Density : The density of fluid rises with nanoparticle inclusion because nanoparticles are denser than the base fluid.
- Boiling point : Nanoparticles raise the fluid's boiling point owing to increased specific heat capacity and thermal conductivity, which enable better heat dissipation.
- Heat transfer coefficient : Introducing nanoparticles enhances the fluid's heat transfer coefficientt. This improvement results from nanoparticles promoting more effective thermal energy exchange between the fluid and its surroundings.

Nanoparticles	**ρ (kg/m^3)**	**Cp (J/kg.K)**	**k (W/m.K)**
Silver (Ag)	10500	235	429
Copper(Cu)	8933	385	401
Aluminium oxide (Al2O3)	3970	765	40
Copper Oxide (CuO)	6320	531.8	76.5
Titanium Oxide (TiO2)	4250	686.2	8.9538

Table 2.1: listing some common properties of selected nanoparticles

The above table is taken from (Sowmya Tippa, Marneni Narahari and Rajashekhar Pendyala, 2016).

2.4.1 Selection of Al_2O_3 Nanoparticle

1. High Thermal Conductivity : Al_2O_3 (aluminum oxide) nanoparticles have a high Thermal conductivity of Al_2O_3 (aluminum oxide) nanoparticles are high compared to many other materials, making them effective for improving the thermal properties of base fluid.
2. Chemical Stability : Al_2O_3 is chemically inert and stable, ensuring that it does not react with the base fluid or corrode the system components. This stability is crucial for maintaining the long-term performance of the nanofluid.

3. Cost-Effectiveness : Al_2O_3 nanoparticles are relatively inexpensive compared to other high-performance nanoparticles like gold or carbon nanotubes, making them a cost-effective choice for large-scale applications.
4. Availability and Ease of Production : Al_2O_3 nanoparticles are readily available and can be produced at a large scale with consistent quality. This ensures that the nanofluid can be reliably produced and utilized.
5. Compatibility with Base Fluids : Al_2O_3 nanoparticles can be effectively dispersed in water and other common base fluids with appropriate surfactants or ultrasonic agitation, ensuring a stable suspension.
6. Research and Application History : Al_2O_3 has been extensively studied and used in various heat transfer applications. This wealth of research provides a solid foundation of knowledge and data, facilitating the design and optimization of experiments.

The base fluid is choosen depending on the specific application requirements, such as temperature range, heat transfer rate, and compatibility with the system components. For example, water-based nanofluids are widely employed in cooling applications because of their high heat transfer rate and low viscosity, whereas oil-based nanofluids are favored for high-temperature applications owing to their superior thermal stability.

2.4.2 Synthesis of nanoparticle Methods

The synthesis of Aluminium oxide nanoparticle can be used by using variety of method.

1. Sol-gel method
2. Vapor phase reaction
3. Hydrothermal method
4. Mechanical milling method
5. Combustion and Precipitation

2.4.3 Sol Gel Method

A sol refers to a colloidal dispersion where particles are extremely small, rendering gravitational forces negligible and relying instead on Van der Waals forces and surface charges.

A gel forms as a semi-rigid mass when the solvent from the sol evaporates, causing particles or ions to aggregate into a continuous network.

Therefore, the sol-gel method is commonly used to achieve precise control over the stoichiometry and morphology of nanoparticles. It is favored and extensively studied because it enables the production of nanoparticles with high purity and a large specific surface area.

2.4.4 Synthesis of Aluminum Oxide Nanoparticles:

The synthesis of aluminum oxide nanoparticles often employs the sol-gel method due to its cost-effectiveness, ability to control particle characteristics, and lower temperature requirements. This chemical technique is particularly advantageous for generating metallic oxides, ceramics, and glass materials. It employs metal alkoxides or inorganic salts as precursors, undergoing hydrolysis and polycondensation reactions to produce a colloidal suspension called a sol. Sol-gel process involves transitioning a liquid "sol" into a solid "gel" phase. Resulting "gel" is subsequently dried and subjected to calcination at varying temperatures to yield the desired metal oxide nanopowder. (Joseph Owalabi and Pius Ojadi, 2023)

2.4.5 Procedure for synthesis of Aluminium oxide nanoparticles:

10 grams of aluminum nitrate nonahydrate ($Al(NO_3)_3 \cdot 9H_2O$) were dissolved in 100 milliliters of pure water to form aluminum nitrate nonahydrate solution. Additionally, 3.35 grams of ethanol were dissolved in 50 milliliters of distilled water to create a solution of ethanol. The synthesis process commenced by stirring the aluminum nitrate nonahydrate solution and the ethanol solution together at room temperature for approximately ten minutes, ensuring the formation of a homogenous mixture. The mixture was subsequently heated to 80°C for one hour to yield a viscous liquid. The

temperature was further elevated to 350°C, and combustion occurred over a span of 45 minutes, leading to a significant evolution of gases and a voluminous reaction.

The resulting burned materials were subsequently ground and subjected to calcination in a muffle furnace for one hour at 1000°C, resulting in the formation of aluminum oxide (Al2O3) nanoparticles (Joseph Owalabi and Pius Ojadi, 2023).

2.5 Characterization using XRD(X-Ray Diffraction)

XRD analysis was employed for characterization of the synthesized aluminum oxide nanoparticles. This technique offers insights into the lattice structure of crystalline substances, providing information about chemical composition, bond angles, unit cell dimensions, and crystallographic structure of materials. The basis of this method lies in the X-rays constructive interference when interacting with crystalline samples.

2.5.1 Bragg's Law and Analysis

X-ray beams produced by a cathode ray tube (CRT) were filtered, collimated, and aimed at the sample. The interaction between these X-rays and the sample led to constructive interference in accordance with Bragg's law, which relates radiation wavelength, diffraction angle, and lattice spacing. Bragg's law is expressed as:

$$n\lambda = 2d\sin\theta \quad \ldots\ldots\ldots\ldots\ldots\ldots\ldots\ldots\ldots\ldots\ldots\ldots\ldots\ldots\ldots\ldots\ldots\ldots\ldots\ldots\ldots\ldots\ldots\ldots\ldots(2.1)$$

Where :

λ = wavelength of X-ray,

n = integer,

θ = glancing angle.

d = perpendicular distance between lattice planes,

2.5.2 Particle size Analysis using XRD Data

The Scherrer's formula was employed to calculate the particle size based on the broadening of X-ray diffraction lines (β) corresponding to specific (hkl) reflections (Joseph Owalabi and Pius Ojadi, 2023).

$$D = \frac{K\,\lambda}{\beta cos\theta} \quad \ldots\ldots\ldots\ldots\ldots\ldots\ldots\ldots\ldots\ldots\ldots\ldots\ldots\ldots\ldots\ldots\ldots\ldots\ldots\ldots\ldots\ldots\ldots\ldots(2.2)$$

Where:

D = Particle size (nm)

λ = 0.15406 nm (X-ray wavelength)

K = 0.9

θ = Peak position (radian)

β = Full Width at Half Maximum , FWHM (radian)

The particle size (D) can be smaller or equal to grain size. Diffraction patterns were recorded using Cu Kα radiation (λ = 1.5418 Å).

2.6 Preparation of Nanofluid

The procedure for preparation of Nanofluid :

- Mass of Al2O3 nanoparticles are measured using a digital electronic balance.
- Gradually introduce the measured Al2O3 nanoparticles into distilled water while continuously agitating the mixture.
- Utilize an ultrasonicator device (400W, 24 kHz) to sonicate the mixture continuously for one hour. This step ensures the nanoparticles are uniformly dispersed in the water.
- Nanofluid can be prepared at varying concentrations, such as 0.2% and 0.4%.

2.7 Mathematical Calculations

The mathematical calculations used in this research work to calculate properties of Al2O3-water nanofluid and overall heat transfer coefficient are shown.

2.7.1. Physical properties

Physical properties of the Al2O3-water nanofluid are calculated based on the proportion of Al2O3 nanoparticles to water, following the method described by M. Fares e.al., 2020.

2.7.2. Density

Density of the Al2O3-water nanofluid (ρnf) is calculated using the mixture rule, which takes under account densities of base fluid (ρbf) and nanoparticles (ρnp). Calculation is as follows:

$$\rho_{nf} = \phi\rho_{np} + (1-\phi)\rho_{bf} \quad \ldots\ldots\ldots\ldots\ldots\ldots\ldots\ldots\ldots\ldots\ldots\ldots\ldots\ldots\ldots\ldots\ldots.(2.3)$$

ϕ = proportion of Al2O3 nanoparticle in water.

Density of Al2O3 nanoparticle is assumed to be independent of temperature within the operating range. Conversely, the density of water varies with temperature. The change in water density, while keeping a flow rate constant, influences the computed heat transfer between the cold and hot side of the heat exchanger.

2.7.3. Specific heat Capacity

Similarly, the specific heat capacity of the nanofluid is determined by the proportions of Al2O3 nanoparticles and water.

$$(\rho Cp)_{nf} = \phi\,(\rho Cp)_{np} + (1-\phi)(\,\rho Cp)_{bf} \quad \ldots\ldots\ldots\ldots\ldots\ldots\ldots\ldots\ldots(2.4)$$

2.7.4. Thermal conductivity

Various models in the literature provide methods for predicting thermal conductivity of nanofluids. These models consider numerous factors, including the thermal conductivities of both the base fluid and the nanoparticles, the surface area and geometry of the nanoparticles, their fractions, and the temperature. Maxwell model is employed to predict the thermal conductivity of Al2O3-water nanofluid.

$$k_{nf} = \frac{k_{bf}\,(k_{np} + 2k_{bf} + 2\phi\,(k_{np} - k_{bf}))}{(k_{np} + 2k_{bf} - \phi\,(k_{np} - k_{bf}))} \quad \ldots\ldots\ldots\ldots\ldots\ldots\ldots\ldots\ldots\ldots\ldots\ldots(2.5)$$

k_{bf} , k_{nf} and k_{np} represents the thermal conductivities of base fluid, nanofluids and nanoparticles, respectively.

2.7.5. Overall heat transfer coefficient

The overall heat transfer coefficient of heat exchanger is determined using the following:

$$U = \frac{Q}{A \times LMTD} \quad \ldots\ldots\ldots\ldots\ldots\ldots\ldots\ldots\ldots\ldots\ldots\ldots\ldots\ldots\ldots\ldots\ldots\ldots\ldots\ldots\ldots \quad (2.6)$$

Where,

LMTD = logarithmic mean temperature difference (K).

$$Q_h = V\,(\rho Cp)_{bf}\ (T_{h1} - T_{h2}) \quad \ldots\ldots\ldots\ldots\ldots\ldots\ldots\ldots\ldots\ldots\ldots\ldots\ldots \quad (2.7)$$

$$Q_c = V\,(\rho Cp)_{nf}\ (T_{c2} - T_{c1}) \ldots\ldots\ldots\ldots\ldots\ldots\ldots\ldots\ldots\ldots\ldots\ldots\ldots\ldots \quad (2.8)$$

$$Q = \frac{Q_h + Q_c}{2} \ldots\ldots\ldots\ldots\ldots\ldots\ldots\ldots\ldots\ldots\ldots\ldots\ldots\ldots\ldots\ldots\ldots\ldots\ldots\ldots\ldots\ldots \quad (2.9)$$

$$LMTD = \frac{(T_{h1} - T_{C2}) - (T_{h2} - T_{C1})}{ln((T_{h1} - T_{C2})/(T_{h2} - T_{C1}))} \quad \ldots\ldots\ldots\ldots\ldots\ldots\ldots\ldots\ldots\ldots \quad (2.10)$$

2.8 Nanofluid Properties

The properties of different concentration of Al2O3-water nanofluid and pure water are given in table 2.2. (Akyurek et al., 2018)

Fluid	**ρ (kg/m^3)**	**Cp (J/kg.K)**	**k (W/m.K)**	**μ (Pa.s)**
Pure water	998	4182	0.598	0.001
0.2% Al_2O_3-Water	1004	4155	0.600	0.00244
0.4% Al_2O_3-Water	1010	4128	0.602	0.00314

Table 2.2: Properties of nanofluid

CHAPTER THREE: MATERIALS AND METHOD

3.1 Research Methodology

The following research methodology will be employed for this thesis work. Each section has been briefly explained.

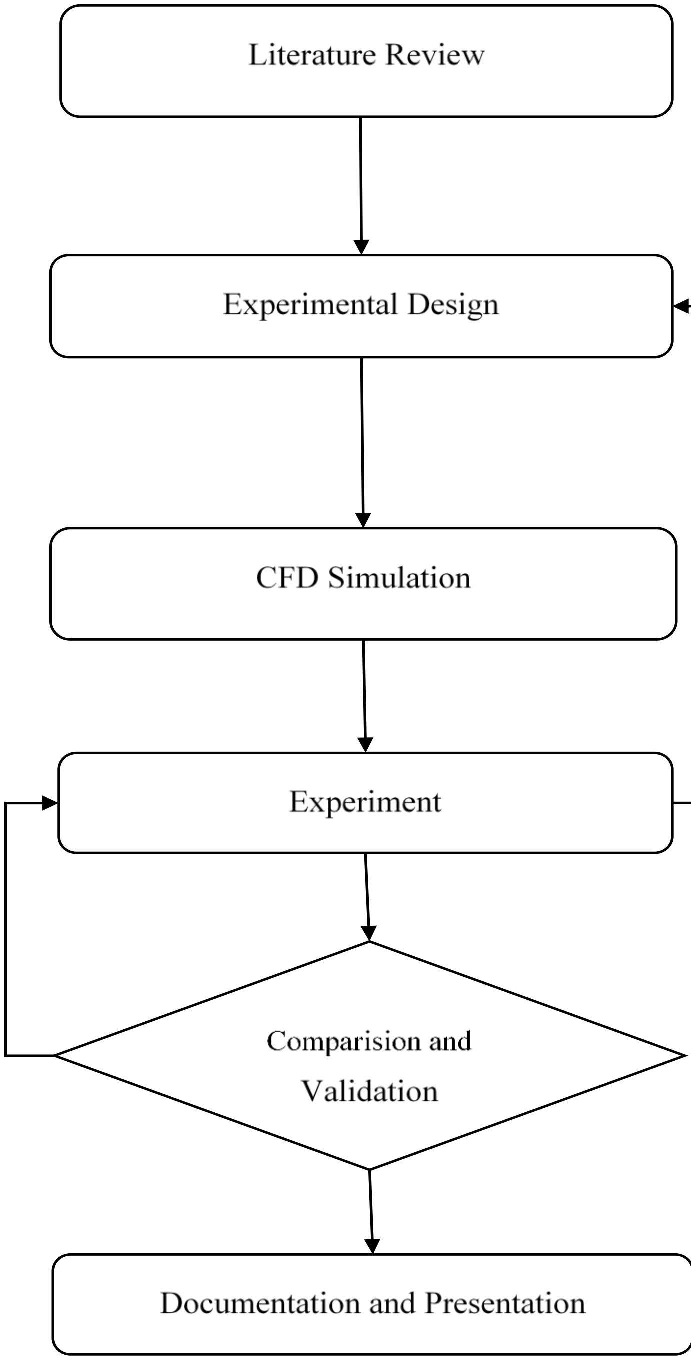

Figure 3.1: Research methodology flow chart

1. Literature Review : A comprehensive review is conducted on existing literature to identify the research gaps and formulate the research objectives.
2. Experimental Design : The experimental setup is designed based on the research objectives. This includes selecting the nanofluid type and concentration, the turbulated tube geometry, and the measurement techniques for heat transfer and fluid flow.
3. Experimental Procedure: The experiment is conducted according to the designed setup, with careful control of the experimental parameters and accurate measurement of the data.
4. CFD Simulation: CFD simulations are conducted to model fluid flow and heat transfer in the turbulated tube. The experimental data is validated against the results obtained from CFD simulations.
5. Conclusion: The findings of the experiment and numerical simulation are summarized, and conclusions are drawn regarding the heat transfer and fluid flow characteristics of nanofluid in turbulated tubes. Recommendations for future research are also provided.
6. Presentation and Documentation: The results and findings of this research will be documented and presented according to the guidelines set forth by the Department of Aerospace and Mechanical Engineering.

3.2 Synthesis of Aluminium Oxide Nanoparticle

10 gram of aluminum nitrate nonahydrate ($Al(NO_3)_3 \cdot 9H_2O$) were dissolved in 100 milliliters of distilled water to form aluminum nitrate nonahydrate solution. Additionally, a solution of ethanol was prepared by dissolving 3.35 grams of ethanol in 50 milliliters of distilled water. The synthesis process commenced by stirring the aluminum nitrate nonahydrate solution and the ethanol solution together at room temperature for approximately ten minutes, ensuring the formation of a homogenous mixture. The mixture was subsequently heated to 80°C for one hour to yield a viscous liquid. The temperature was further elevated to 350°C, and combustion occurred over a span of 45 minutes, leading to a significant evolution of gases and a voluminous reaction.

The resulting burned materials were subsequently ground and subjected to calcination in a muffle furnace for one hour at 1000°C, resulting in the formation of aluminum oxide (Al2O3) nanoparticles.

3.3 Preparation of Nanofluid

The procedure for preparation of Nanofluid :

- Mass of Al2O3 nanoparticles are measured using a digital electronic balance.
- Gradually introduce the measured Al2O3 nanoparticles into distilled water while continuously agitating the mixture.
- Utilize an ultrasonicator device (400W, 24 kHz) to sonicate the mixture continuously for one hour. This step ensures the nanoparticles are uniformly dispersed in the water.
- Nanofluid can be prepared at varying concentrations, such as 0.2% and 0.4%.

Figure 3.2: Preparation of nanofluid

3.4 Experimental Setup

The experimental setup comprises three primary components: the primary heat exchanger, the data acquisition system and the water bath section, as shown schematically in the figure 3.3. The main test loop includes a pump, flow sensor, pressure gauge, Arduino UNO, K-type thermocouple, computer, power supply unit, and the heat exchanger. The test section consists of shell and tube heat exchanger. Tube is made of Aluminium material and shell is made of PPR pipe . The external and internal diameter of shell were 40mm and 32mm respectively. External and internal diameter of tube were 15mm and 13mm respectively and a wall thickness of 1mm. The total length of test section is 1180mm.

Two K-type thermocouples are installed at both ends of the aluminum pipe with a diameter of 2.5mm, and two more are placed at both ends of the PPR pipe to measure inlet and outlet temperatures of cold and hot fluid, respectively. These K-type thermocouple was calibrated in a thermostat with a deviation of ±0.1 °C before use. Temperature readings were recorded via a computer connected to an Arduino, with the average values used for analysis. Heat transfer from the hot fluid increases the temperature of cold fluid, consequently decreasing temperature of the hot fluid.

An additional heat exchanger is utilized to maintain the cold fluid at a constant inlet temperature. The water tank of 24 L (46x23x23 cm) is used. An electrical geyser heats the hot fluid, keeping the temperature steady at 68 °C. A pressure gauge measures the pressure across test section. A pump is used to circulate hot fluid through outer side of tube, while the flow rate of hot and cold fluid is measured by a flow sensor.

To examine the effects on pressure drop and heat transfer, two types of turbulators with pitches of 16mm and 20mm and each measuring 1000mm in length are used in a shell and tube heat exchanger. These turbulators were designed to be inserted into the testing area through removable elements located at both ends of the shell and tube heat exchanger.

For this experiments, a nanofluid was circulated through the system by a pump. Hot water at 68 °C then flows through outer side of tube. The flow rates of both the nanofluid and th hot water were adjusted accordingly, with the hot water inlet flow rate set at 132 l/hr and the cold water inlet flow rate varying between 470 and 620 l/hr. As the Al2O3-water nanofluid flowed through the tube, its temperature increased. Once a steady state was reached, the temperatures of both the nanofluid and the hot water were measured.

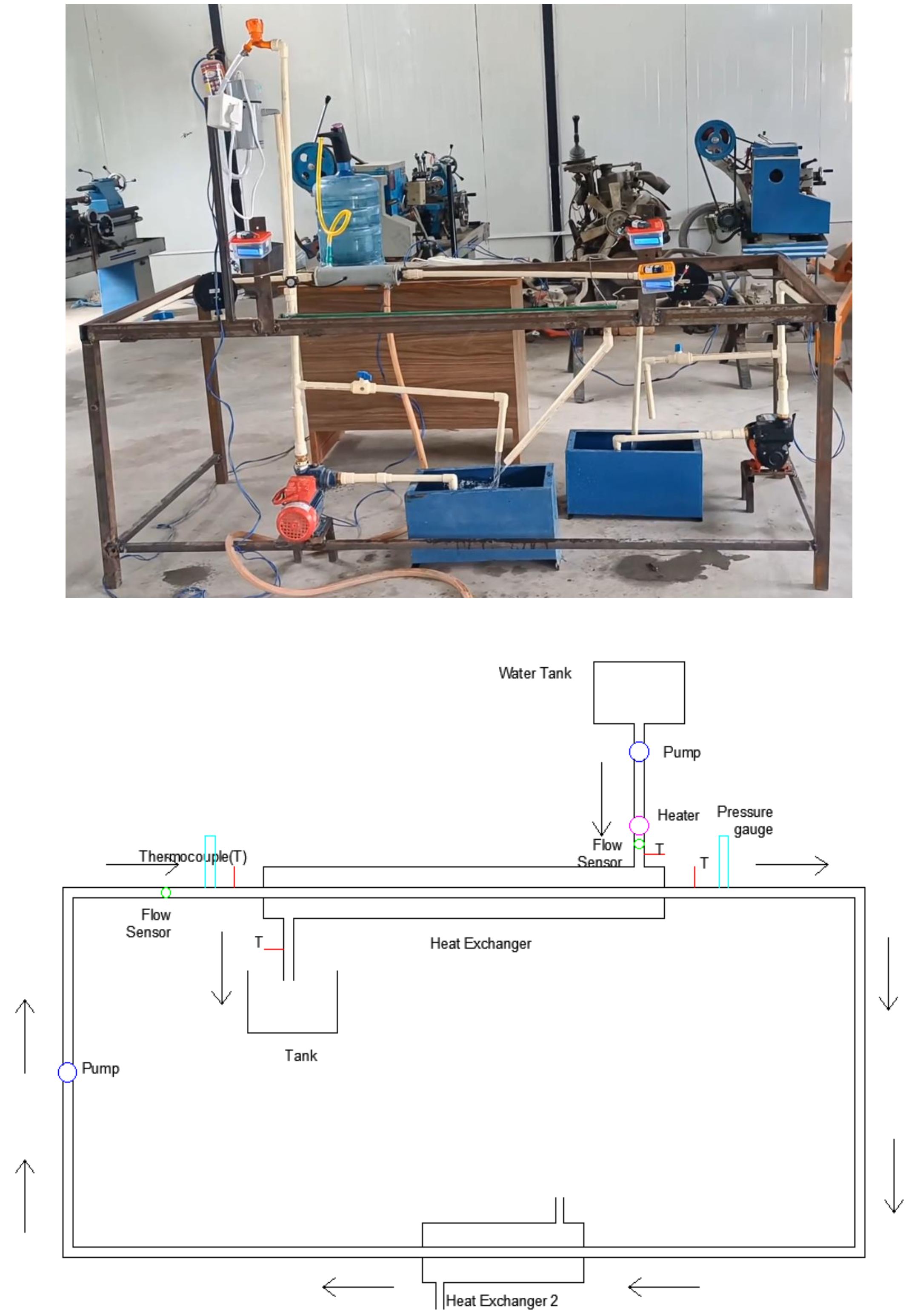

Figure 3.3: Experimental Setup

3.5 Construction of Heat Exchanger

Shell and tube heat exchanger was made for this research work. Shell is made of PPR pipe and Tube is made of Aluminium material. The external and internal diameter of shell were 40mm and 32mm respectively. External and internal diameter of tube were 15mm and 13mm respectively .

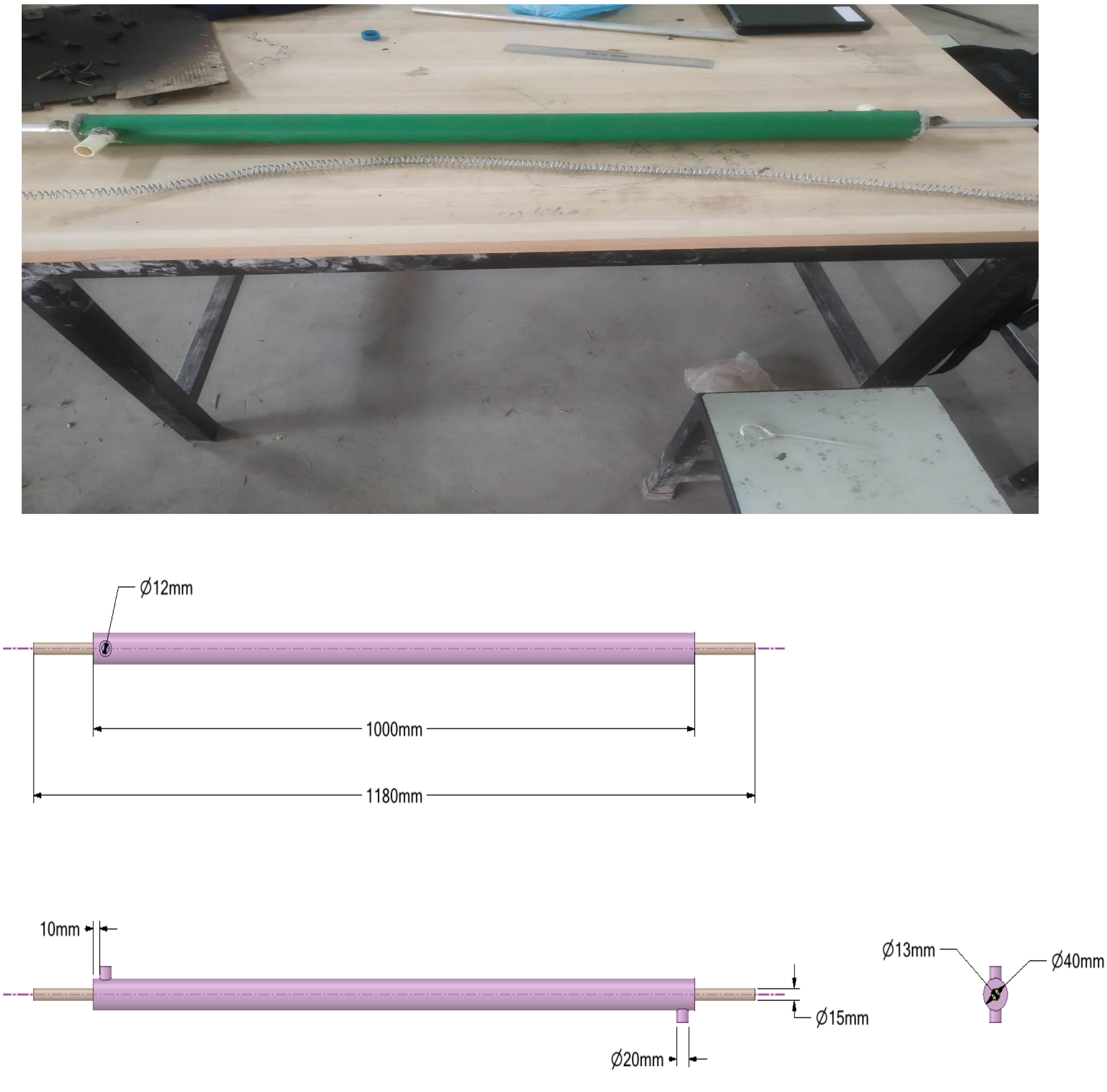

Figure 3.4: Heat Exchanger

3.6 Fabrication Procedure

The fabrication of the heat exchanger was a crucial aspect of preparing the experimental setup for this research. High-quality fabrication was essential to achieve accurate and reliable experimental results. Figure 3.5 illustrates the various steps involved in the fabrication process.

Figure 3.5: Fabrication procedure

The fabrication involved various steps are as follows:

1. Support structure fabrication: Support structure fabrication began with square and rectangular pipes composed of mild steel. These pipes were measured, cut, and welded to fit the dimensions required for supporting the experimental setup

2. Heat exchanger fabrication : Shell and tube heat exchanger was made for conducting experiment. Shell is made of PPR pipe and Tube is made of Aluminium material.

3. Joining of cpvc pipe fittings : To flow hot and cold fluid cpvc pipe was used . All the fittings are of cpvc material .

4. Making Turbulator : Two helical coil turbulator was made up of mild steel material.

5.Connection of hydraulic pump: Two Hydraulic pump of capacity 0.37 KW power is installed and connected to inlet side of shell and tube for continous flow fluid.

6. Connection of geyser : Geyser is connected to inlet side of shell after pump for continuously supply hot water to the exchanger.

7. Connection of pressure gauge : Pressure gauge is connected to the outlet and inlet side of tube to measure pressure.

8. Connection of Flow sensor : Flow sensor is connected to the inlet side of both tube and shell to measure the flow rate.

9. Connection of Thermocouple : Four thermocouple was used at outlet and inlet side of bot tube and shell to determine temperature.

10. Final Inspection: Check for leakage and further proceeded to experiment.

3.7 Performing Experiment

Experiment was performed at workshop of Shankharapur Polytechnical Institute, Ctevt. Experiment was performed to collect various data for different experiment.

Various data collected are :

1. Temperature : Temperature of both inlet and outlet side of cold and hot fluid was recorded with the help of K-type thermocouple.

2. Flow rate : Cold and hot fluid flow rate was recorded with the help of flow sensor .

3. Pressure : Pressure at inlet and outlet side of tube was recorded with the help of pressure gauge.

3.8 Procedure to perform the experiment

The experimental procedure and data collection steps are as follows:

1. The water is filled in the tank.

2. Ensure all components of the experimental setup are in proper working condition, checking for any leaks, seals, and other potential issues.

3. The thermocouple and flow sensor were connected to the Arduino Uno board to monitor temperature and flow rate.

4. Pump and geyser was started to flow hot and cold fluid.

5. Ball valve was adjusted to obtain desired flow rate.

6. At steady state, Pressure and flow rate was recorded.

7. The reading of the temperature was recorded.

8. Same procedure was repeated for every experiment.

Figure 3.6: Performing Experiment

3.9 Temperature Measurement

The temperatures at the inlets and outlets of the cold and hot fluids can be measured using K-type thermocouples, which are connected to an Arduino UNO and a computer for data collection.

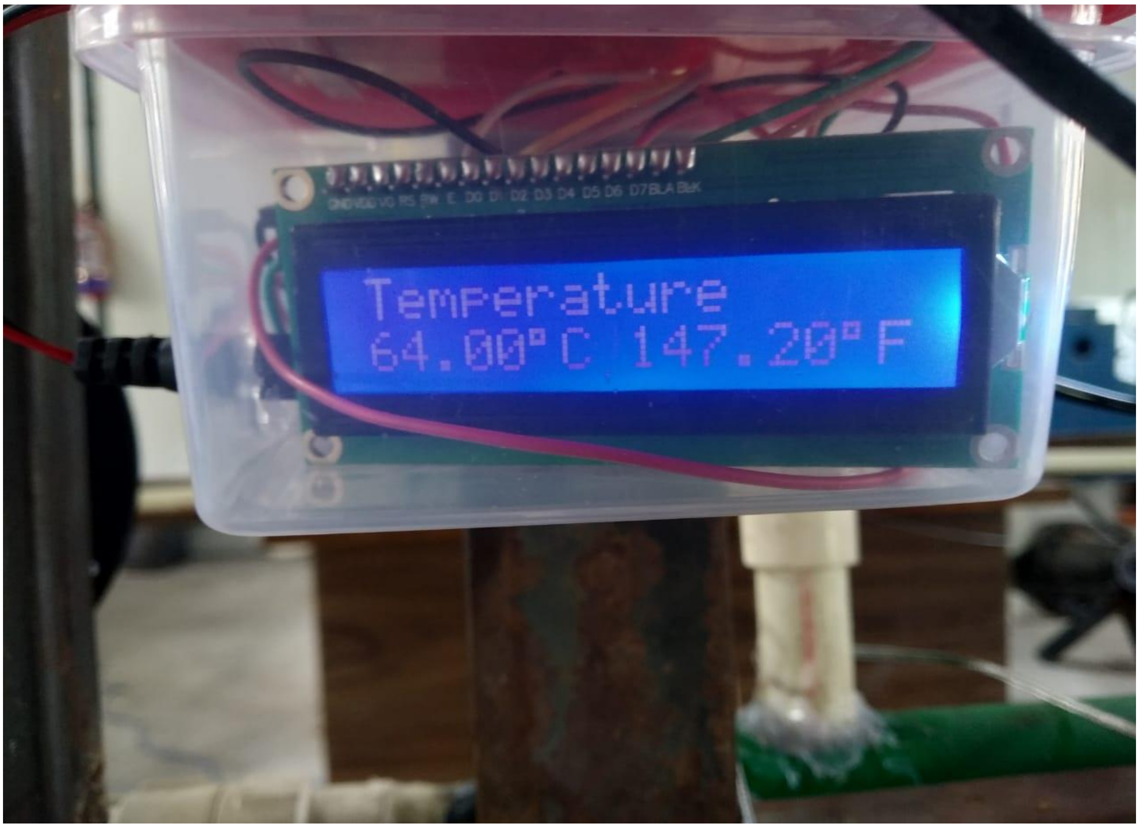

Figure 3.7: Temperature Measurement

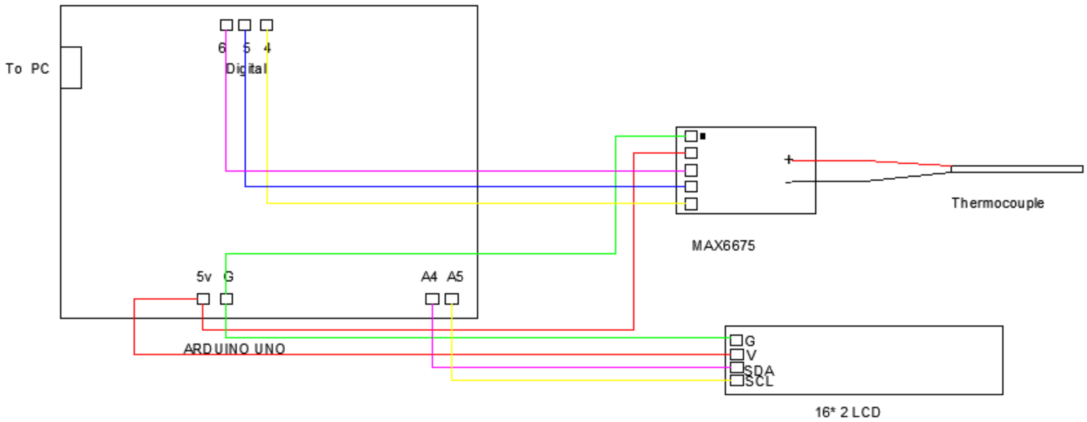

Figure 3.8: Thermocouple Connection Diagram

3.10 Flow Measurement

Inlet Flow rate of cold fluid andhot fluid can be measured by using flow sensor and Arduino UNO connected with computer by Arduino coding.

Figure 3.9: Flow Measurement

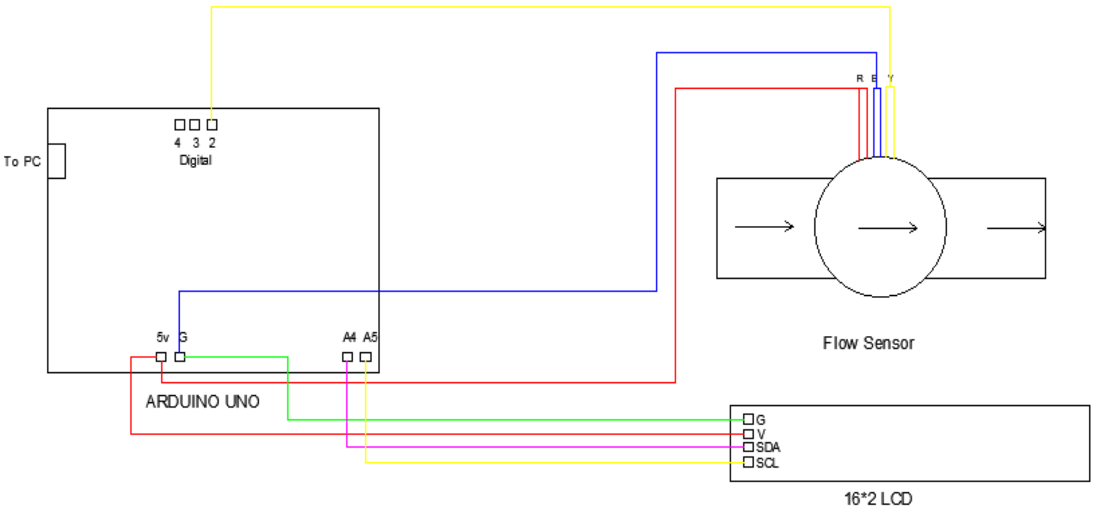

Figure 3.10: Flow Sensor Connection Diagram

3.11 Measurement of Pressure

Pressure at outlet and inlet side of tube was recorded with the help of pressure gauge. Pressure gauge can measure 0 to 1 kg/cm2 pressure.

Figure 3.11: Pressure gauge

3.12 Helical Coil Turbulator

Helical Coil Turbulators are used to create turbulance flow in pipe. Here two different pitch of helical coil are using. Helical coil outer diameter is 12 mm and length of 1000 mm. Diameter of wire is 1 mm. And three different pitches of helical coil are 16 mm and 20 mm.

Figure 3.12: Helical Coil Turbulators

3.13 Materials, equipment and measuring devices

3.13.1 Materials and Equipments:

- **Nanofluids**: These are engineered colloidal suspensions containing nanoparticles dispersed in a base fluid, typically oil, ethylene glycol or water. Aluminium Oxide (Al_2O_3) nanoparticle can be used for this experiment
- **Pipes** : Shell was made of PPR Pipe of external diameter 40mm . Tube was made of Aluminium of external diameter 15mm. And other pipes for circulation of fluid is CPVC material.
- **Mildsteel pipes** : For making support structure of the experiment , square and rectangular mildsteel pipes were used.
- **Hydraulic pump** : Two pumps were used for circulation of hot fluid and cold fluid in shell and tube heat exchanger . The capacity of pump was 0.37 kw.
- **Electric Geyser** : To supply hot fluid to the system , electric geyser was used to heat water . The electric power of geyser was 3000 watt.
- **Heat exchanger** : One main heat exchanger and one secondary heat exchanger were used in this experiment. Secondary heat exchanger was used to maintain temperature of outlet cold fluid.
- **Other fittings** : Other fittings like cpvc L-bow , cpvc Tee , cpvc male and female socket , cpvc Tee socket , cpvc union were used to made experimental setup.

3.13.2 Measuring devices:

- **Flow sensor**: To measure the flow rate of fluid, flow sensor was used.
- **Pressure gauge**: To measure Pressure drop , Pressure gauges were used in this experiment.
- **Temperature Sensors**: To measure temperatures at oulet and inlet of the tube, K-type thermocouples were used.

3.14 Heat Exchanger Modelling

The initial step in conducting a computational fluid dynamics (CFD) analysis involves creating a geometric model of the heat exchanger that includes required design specifications. ANSYS Workbench is utilized for the CFD analysis in this research. The

Design Modular module in ANSYS Workbench offers the necessary tools to develop the model of the problem based on the specified dimensions of geometries.

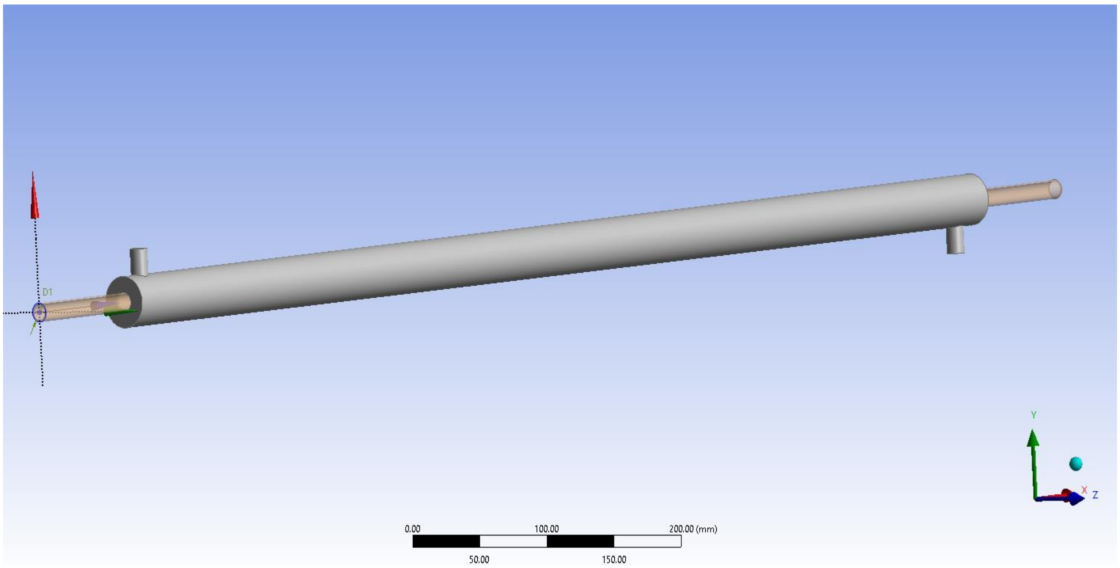

Figure 3.13: Heat Exchanger Modelling

Design Modular, a versatile module in ANSYS Workbench, provide numerous commands and options for creating both 2D and 3D geometries. The 3D model of the heat exchanger, crafted according to the specified dimensions using DesignModular, is illustrated in Figure 3.13

3.15 Meshing

After creating the geometric model, the subsequent stage in the CFD analysis of the heat exchanger involves generating a mesh for the problem domain. Meshing divides the large domain into numerous small cells, applying various relationships and equations to simulate the physical problem using CFD software. The number and size of these cells are crucial as they directly influence the accuracy of the simulation results. For this study, meshing was performed using the default settings in Ansys Fluent.

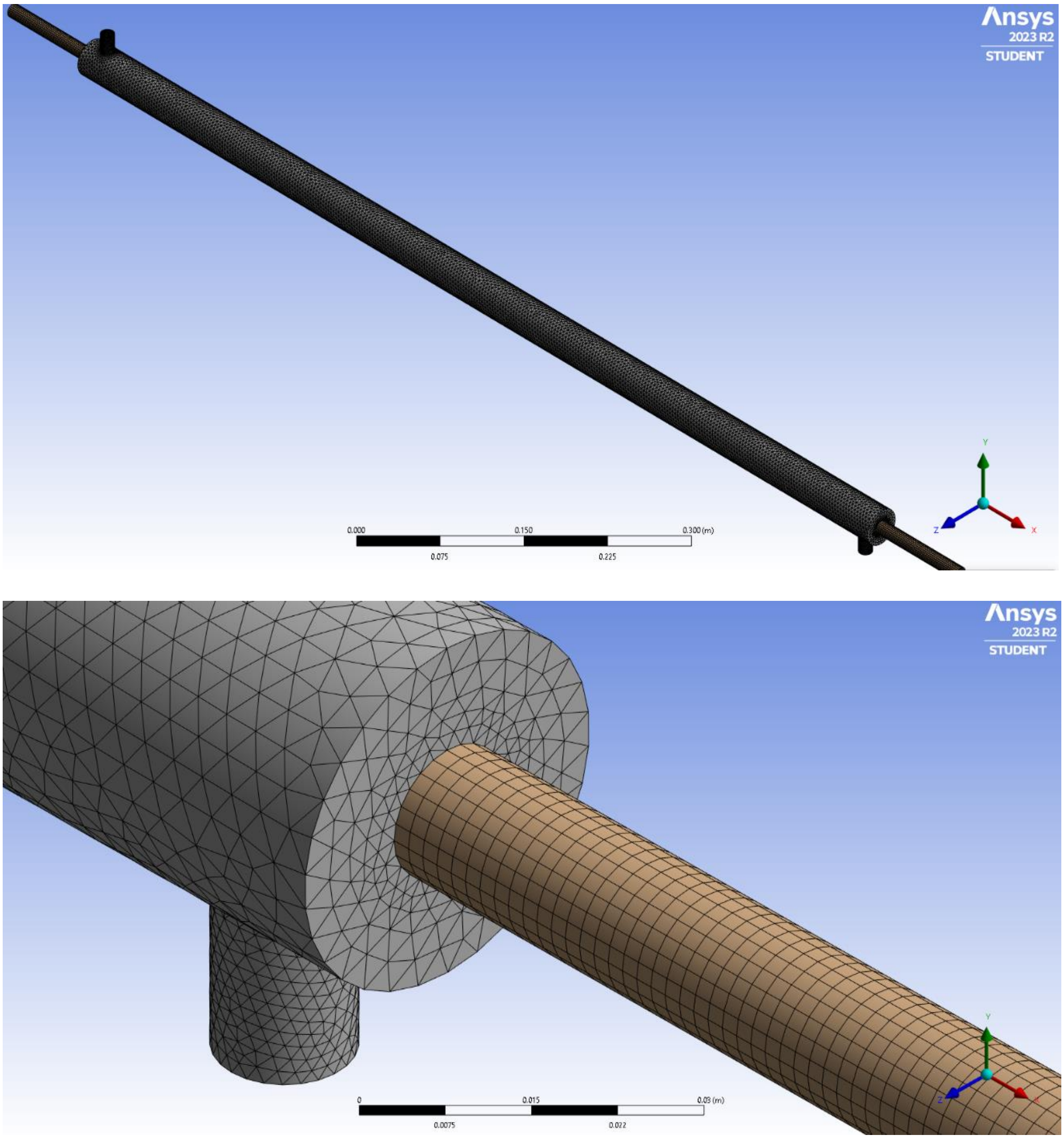

Figure 3.14: Meshing of Heat Exchanger

3.16 CFD simulation of heat exchanger using ANSYS

The CFD simulation of heat exchanger using ANSYS Fluent is facilitated by its Fluid Flow module, which allows for precise heat transfer simulations on specified boundaries and regions within a model. It enables the simulation of various heat transfer mechanisms including convection, conduction, and radiation. This study utilizes CFD to model heat exchanger, focusing on simulating heat transfer between cold and hot fluids inside exchanger. Assumptions have been carefully considered to ensure the reliability and accuracy of the CFD analysis for heat exchanger study.

3.17 Numerical Method Employed

Computational fluid dynamics (CFD) utilizes various numerical methods to discretize the Navier-Stokes equations for simulating fluid flows. The primary methods include:

1. Finite Difference Method (FDM)
2. Finite Volume Method (FVM)
3. Finite Element Method (FEM)
4. Spectral Galerkin Method (SGM)

Among these, FDM and FVM are commonly preferred in commercial CFD packages due to their effectiveness in handling fluid flow problems. In this study, FLUENT has been selected, which employs the Finite Volume Method (FVM) for simulating fluid flow problems.

3.18 Selecting Viscous Model

The current simulation utilizes the k-epsilon turbulence model with the realizable model, incorporating scalable wall functions for this research. Default values are maintained for all other parameters in the simulation setup.

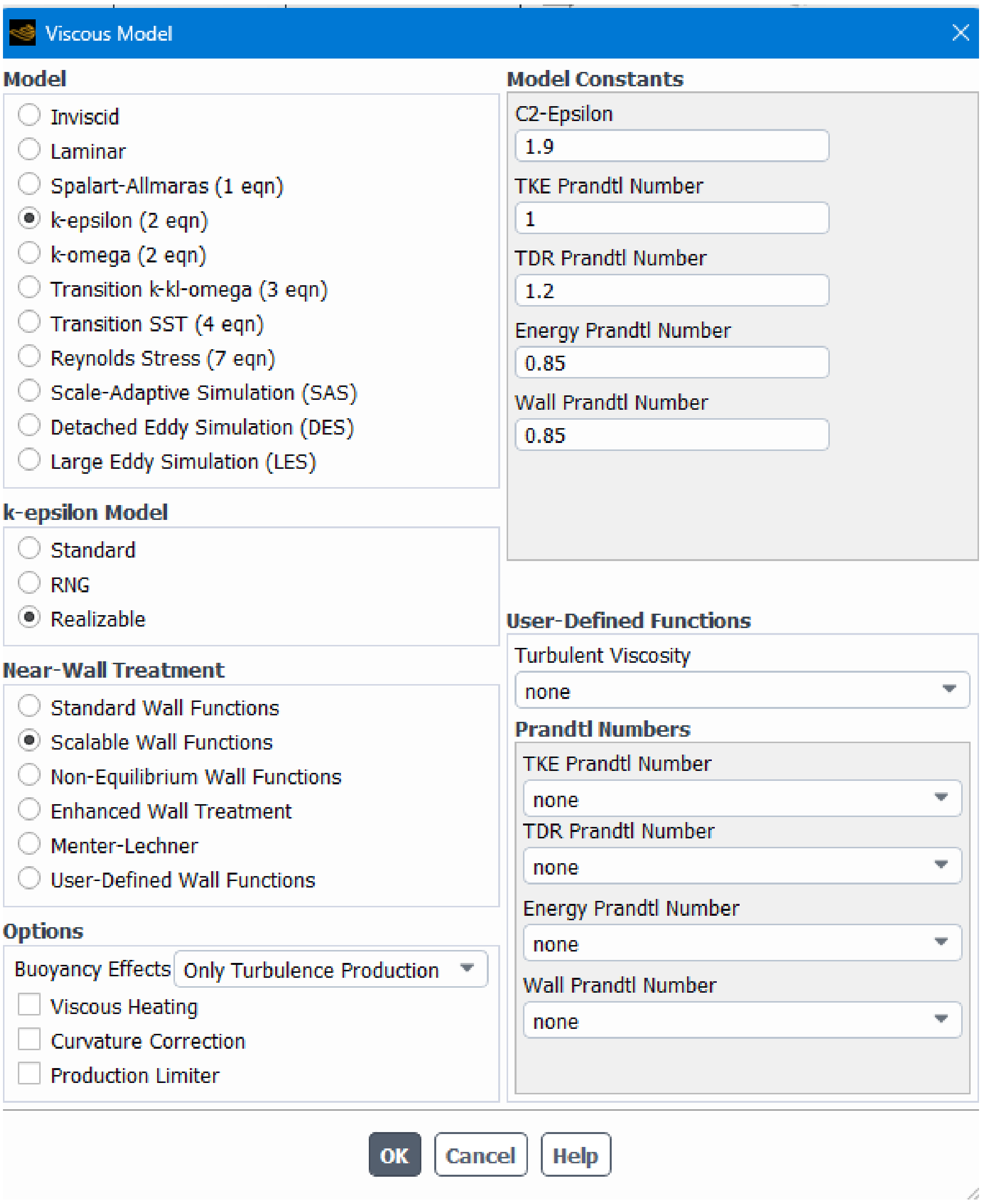

Figure 3.15: Viscous model

3.19 Specifying Materials

Material selection is a crucial parameter for simulation. It plays a significant role in modeling heat transfer process. This research involved both solids and fluids. For the fluids, water was selected from the FLUENT database. For the solids, the materials chosen included aluminum for the tube and ppr for the shell. The data for the ppr and Al2O3-water nanofluid were manually specified, while the properties for the other materials were taken from the FLUENT database.

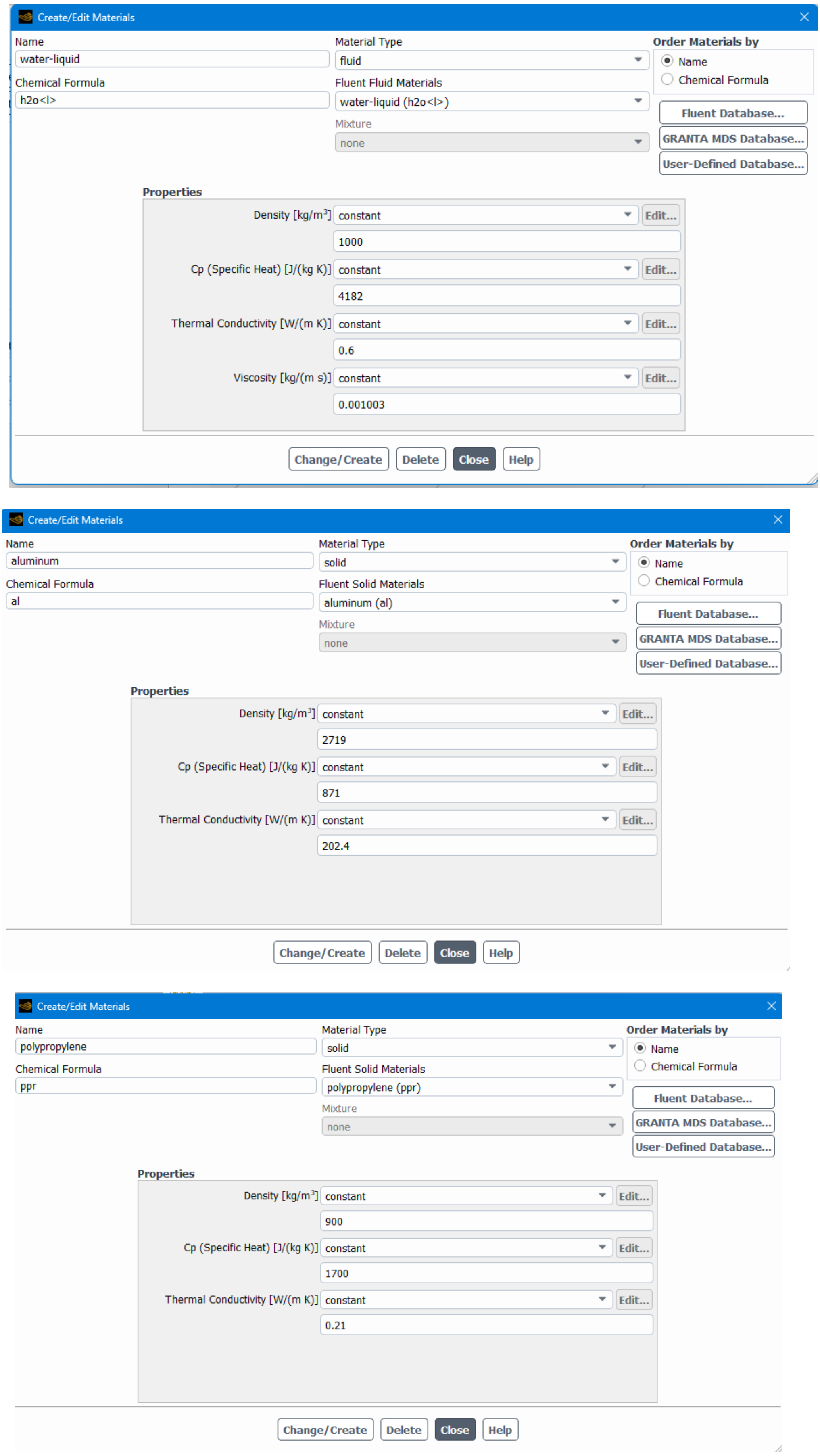

Figure 3.16: Specifying materials

3.20 Specifying Boundary Conditions

Boundary conditions are crucial for accurately simulating any problem domain. The precision and validity of the results rely on the correct specification of these conditions. Most boundary conditions are selected based on practical applications, while others are determined by the simulation software's built-in algorithms. In this section, the boundary conditions for the geometric model are defined for its various components.

Boundary conditions specifying is a crucial step in problem simulation. These conditions generally encompass various constraints related to the problem domain, based on which the solver computes different equations. Physical or practical boundary conditions are translated into terms understandable by the simulation software. The boundary condition for outlet of both tube and shell in the heat exchanger is set as a pressure outlet

Initially, all components were named according to their respective functions for ease of identification. Named selection was used during the naming process. The boundary condition for components of shell and tube heat exchanger are briefly outlined as follows:

- Hot inlet velocity and temperature : and 0.18229 m/s^2 and 68 ˚C
- Cold inlet velocity and temperature : 0.983 , 1.0878 , 1.1923 and 1.297 m/s^2 and 26 ˚C

3.21 Solution Generation Method

ANSYS FLUENT provides two methods for discretizing the solution of governing equations: the 1st order upwind solution method and the 2nd order upwind solution method.

In the 1st order upwind method, the face value of the cell is taken as equal to the central cell value. In contrast, the 2nd order method employs Taylor series expansion to solve the governing equations.

For applications where the highest level of accuracy is not critical, ANSYS FLUENT recommends using the 1st order method due to its lower computational cost. Conversely, the 2nd order method is recommended when the solution requires the highest accuracy, despite the increased computational time (Fluent, 2023).

In this study, the 2nd order upwind solution method was employed to ensure accuracy in the solution of the governing equations.

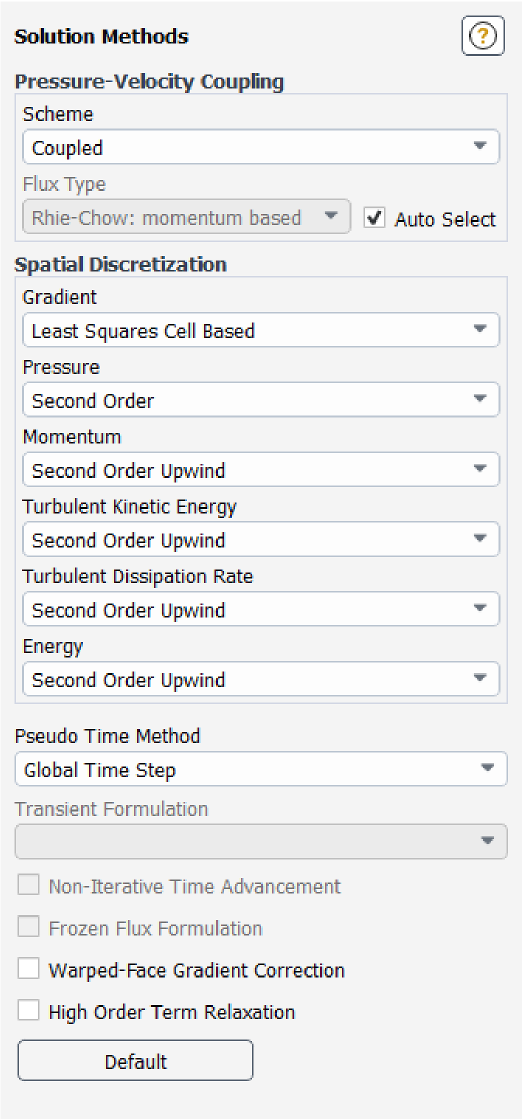

Figure 3.17: Solution Methods

3.22 Solution Initialization

Once all parameters and variables were specified, the solution was initialized. The number of iterations was selected based on computational convenience and time constraints.

CHAPTER FOUR: RESULTS AND DISCUSSION

4.1 CFD Simulation of Heat Exchanger

Heat exchanger was modeled and simulated using CFD, with various parameters and values specified. After initializing the solution, results were obtained in the form of different contour plots.

4.1.1 Pressure Contour

Pressure variations at inlet and outlet sides of the cold fluids are evident in the pressure contour plots. There is pressure drop of cold fluid from inlet to outlet side of heat exchanger.

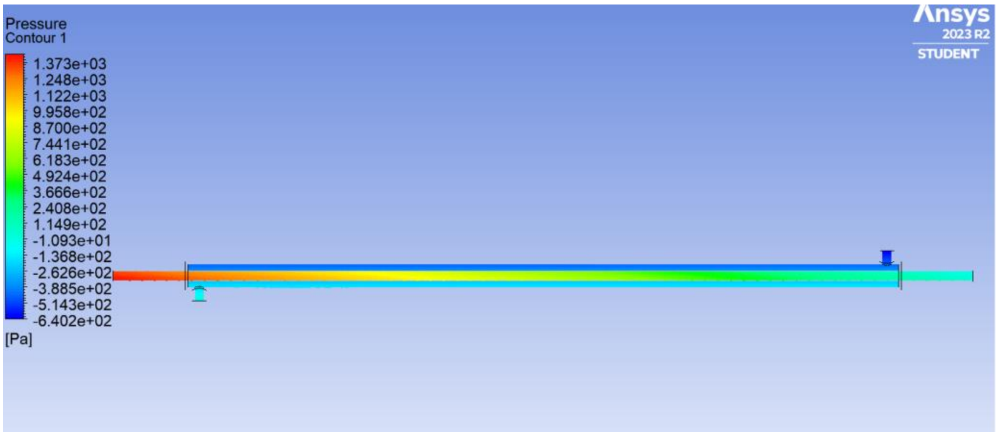

Figure 4.1: Pressure Contour

4.1.2 Tempearture Contour

Temperature increases from inlet side to outlet side of cold fluid inside tube of the heat exchanger , while conversely, the temperature decreases for hot fluid from inlet to the outlet side.

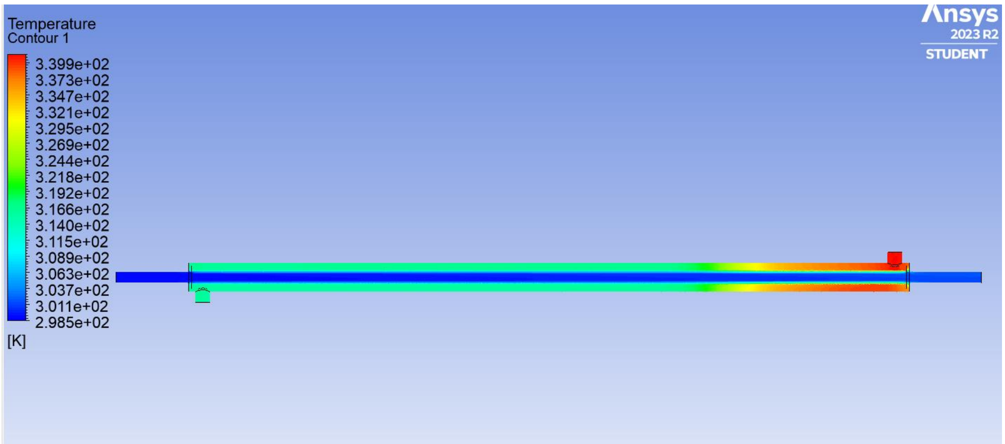

Figure 4.2: Temperature Contour

4.2 Synthesize Al_2O_3 Nanoparticle

The synthesize Al2O3 Nanoparticle are shown in figure 4.3.

Figure 4.3:Synthesize Al2O3 Nanoparticle Sample

4.3 X-Ray Diffraction (XRD)

The Miller Indices obtained from XRD data of Al_2O_3 Nanoparticle are 012 , 104 , 110 , 113 , 024 , 116 , 118 , 024 , 030 and 119 is shown in Figure 4.4 are close to the data obtained by (Joseph Owalabi and Pius Ojadi, 2023) .The average size of nanoparticle obtained was 35 nm.

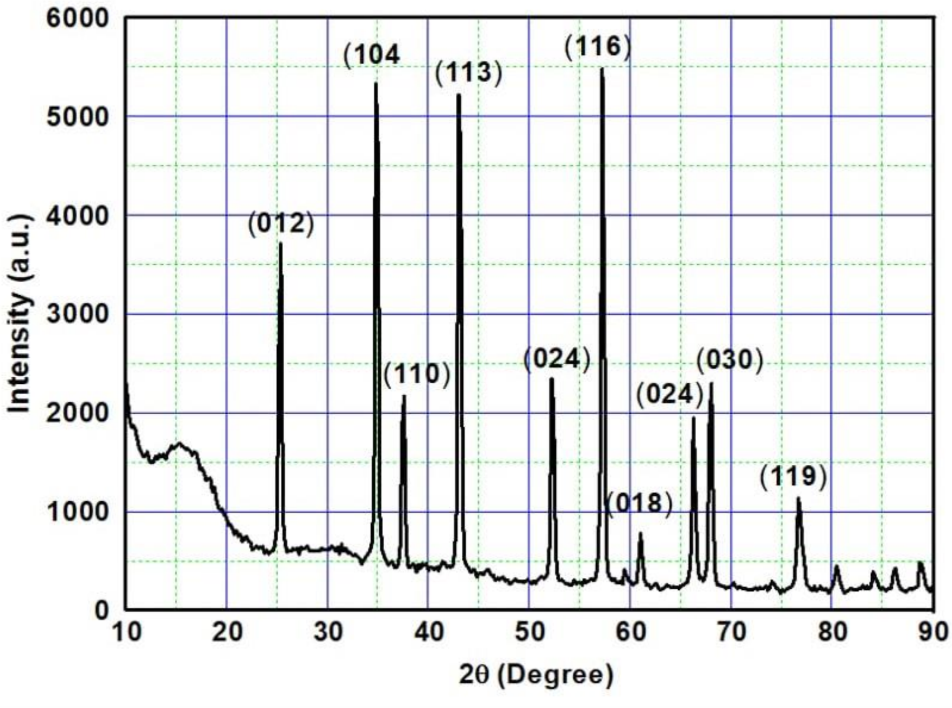

Figure 4.4: X-Ray Diffractogram of Al2O3 Nanoparticle

4.4 Comparision of Overall heat transfer coefficient with different flow rate for different nanofluid concentration

Overall heat transfer coefficients for 0.2% and 0.4% Al_2O_3-water nanofluids without turbulators increase by 11.47% to 19.5% and 20.77% to 34.66%, respectively, across flow rates ranging from 470 to 620 l/hr compare to pure water. This improvement is due to enhanced thermal conductivity and increased surface area provided by the nanoparticles, as reported in previous works on graphene nanofluid concentrations (M. Fares et al., 2020).

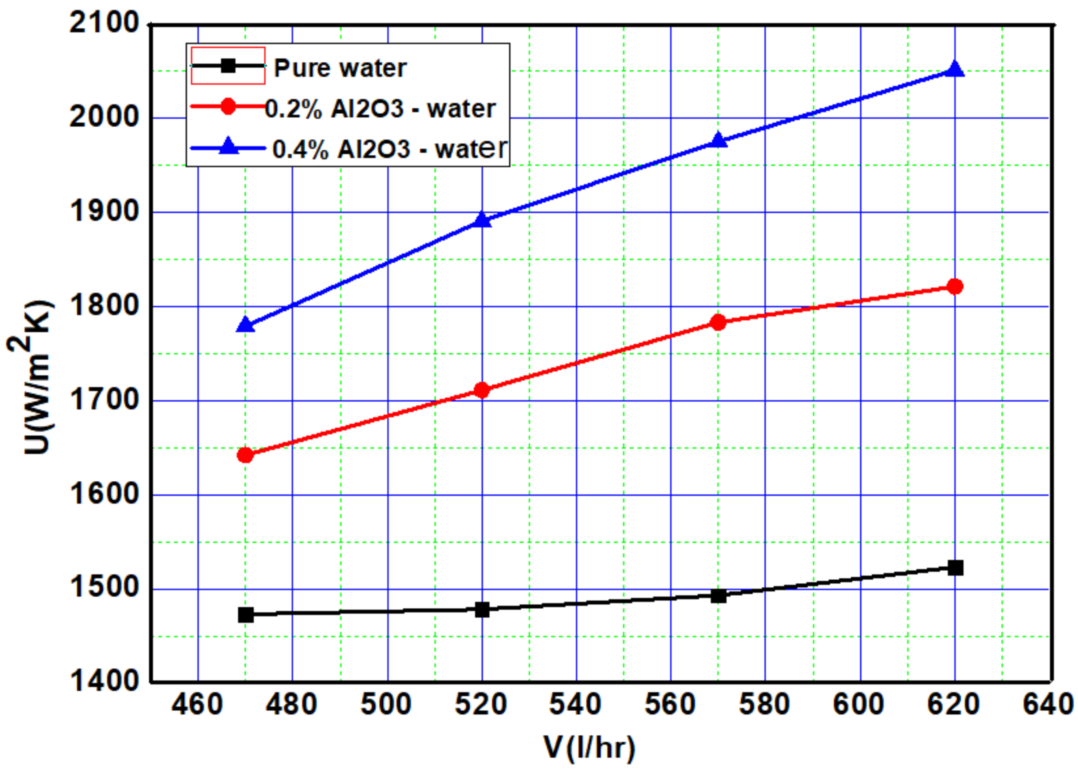

Figure 4.5: Overall heat transfer coefficient vs flow rate for different concentration nanofluid

4.5 Comparision of Overall heat transfer coeffiecient with different flow rate for different turbulators for pure water

Adding a 16 mm helical coil turbulator inside the tube of the heat exchanger, the overall heat transfer coefficient increased by 47.09% to 54.76% compared to pure water without turbulator,as shown in fig 4.6. Similarly, incorporating a 20 mm helical coil turbulator, the overall heat transfer coefficient increased by 26.7% to 34.66% compare to pure water conditions without turbulator. These turbulators create significant turbulence, thereby enhancing heat transfer from the hot water to the nanofluids in the heat exchanger. The helical coil turbulator act as turbulence promoters when in contact with the pipe wall and increases heat transfer. Smaller pitch sizes in the helical coils intensify turbulence, resulting in enhanced heat transfer, consistent with findings in previous literature (Akyürek et al., 2018).

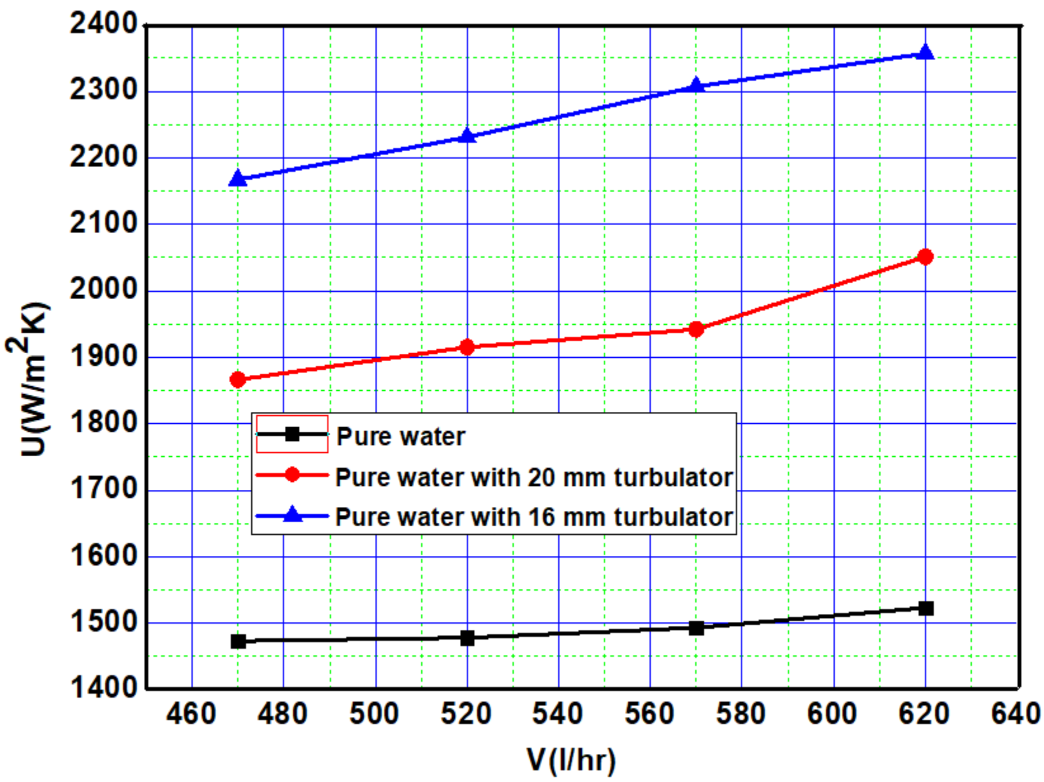

Figure 4.6: Overall heat transfer coefficient vs flow rate for pure water with different turbulator

4.6 Comparision of Overall heat transfer coefficient with different flow rate for 0.2% nanofluid for different turbulator.

Fig. 4.7 illustrates the enhancement in overall heat transfer coefficient of 0.2% Al2O3-water nanofluids with different turbulator. Specifically, using a 16 mm pitch helical coil turbulator in 0.2% Al2O3-water nanofluids ,overall heat transfer coefficient increases from 42.51% to 39.78%, whereas adding 20mm helical coil turbulator in the same nanofluid led to an increase between 20.52% and 21.26% compared to using the nanofluid without any turbulators in the heat exchanger.

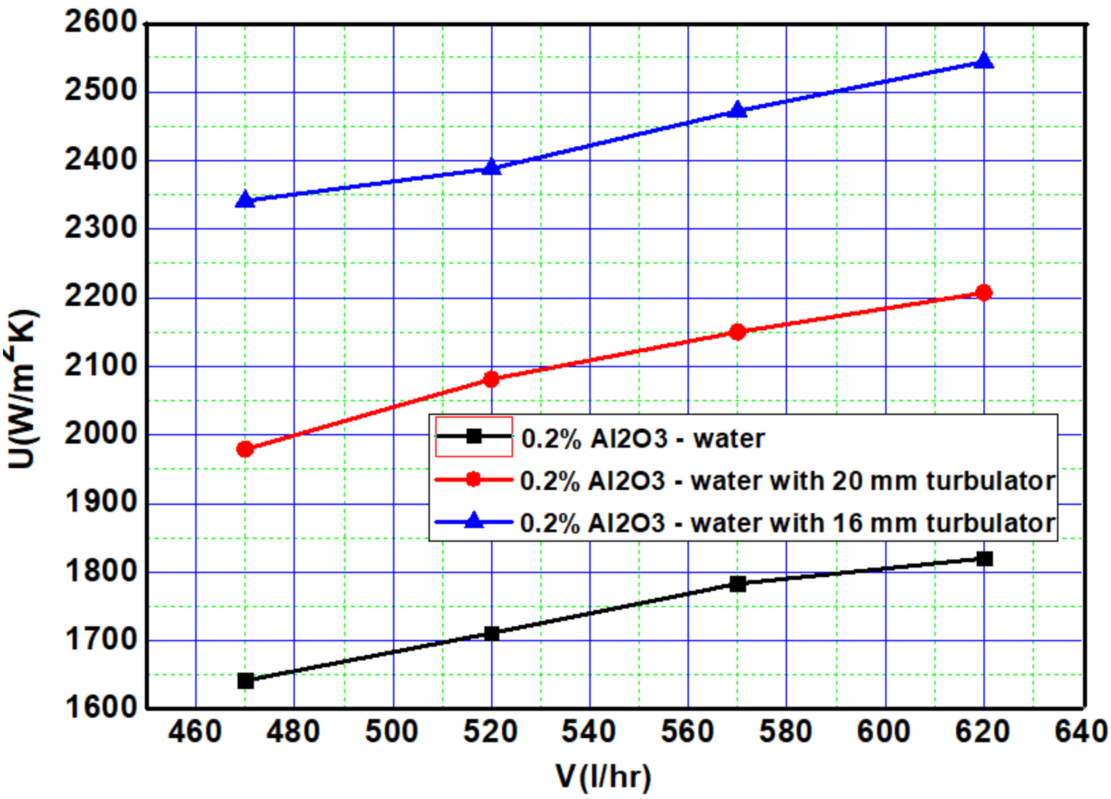

Figure 4.7: Overall heat transfer coefficient vs flow rate of 0.2% nanofluid with different turbulator

4.7 Comparision of Overall heat transfer coefficient with different flow rate for 0.4% nanofluid for different turbulator

Fig. 4.8 illustrates the enhancement in overall heat transfer coefficient of 0.2% Al2O3-water nanofluids with different turbulator. Employing a 16 mm pitch helical coil turbulator in 0.4% Al2O3-water nanofluids, overall heat transfer coefficient increased by 51.48% to 44%. Similarly, adding 20mm helical coil turbulator in the same nanofluid led to an increases by 21.81% to 15.6% compared to using the nanofluid without any turbulators.

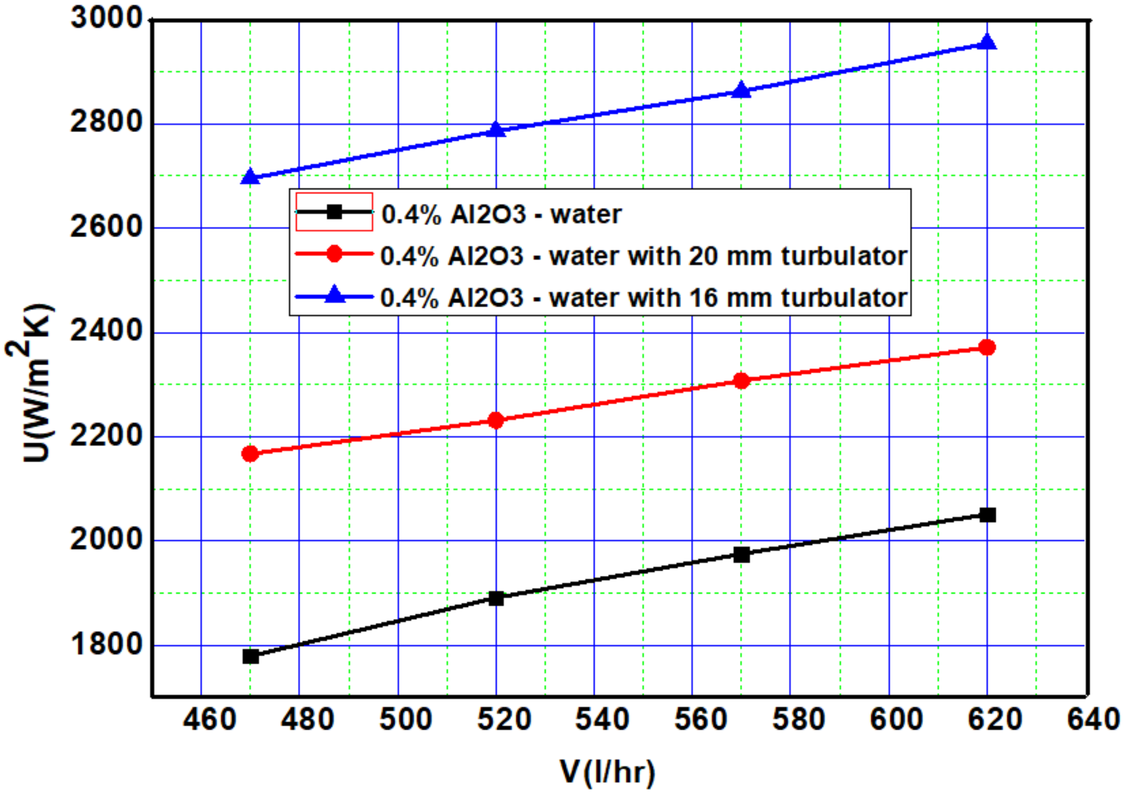

Figure 4.8: Overall heat transfer coefficient vs flow rate of 0.4% nanofluid with different turbulator

4.8 Comparision of Overall heat transfer coefficient with different flow rate for different concentration of nanofluid for 16 mm turbulator

Comparision of the overall heat transfer coefficient of 16 mm pitch helical coil turbulator for pure water and different concentrations of nanofluid are shown in fig.4.9. The use of a 16 mm pitch helical coil with 0.2% and 0.4% nanofluid results in increasing the heat transfer coefficient by 7.93% and 25.32%, respectively, over using a 16 mm trubulator in the case of water.

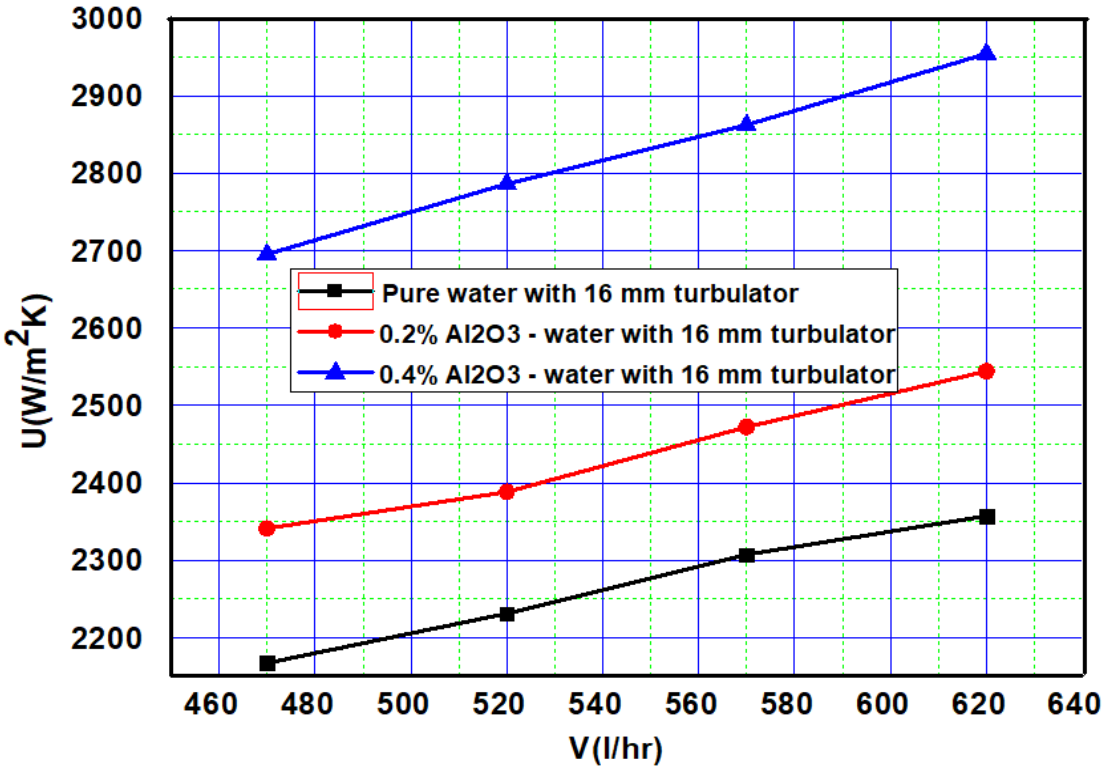

Figure 4.9: Overall heat transfer coefficient vs flow rate for different concentration nanofluid with 16mm turbulator

4.9 Comparision of Overall heat transfer coefficient with different flow rate for different concentration nanofluid for 20 mm turbulator

Comparision of the overall heat transfer coefficient of 20 mm pitch helical coil turbulator for pure water and different concentrations of nanofluid are shown in fig.4.10. The use of a 20mm pitch helical coil with0.2% and 0.4% nanofluid results in increasing the heat transfer coefficient by 7.6% and 15.6%, respectively, over using a 20 mm trubulator in the case of water.

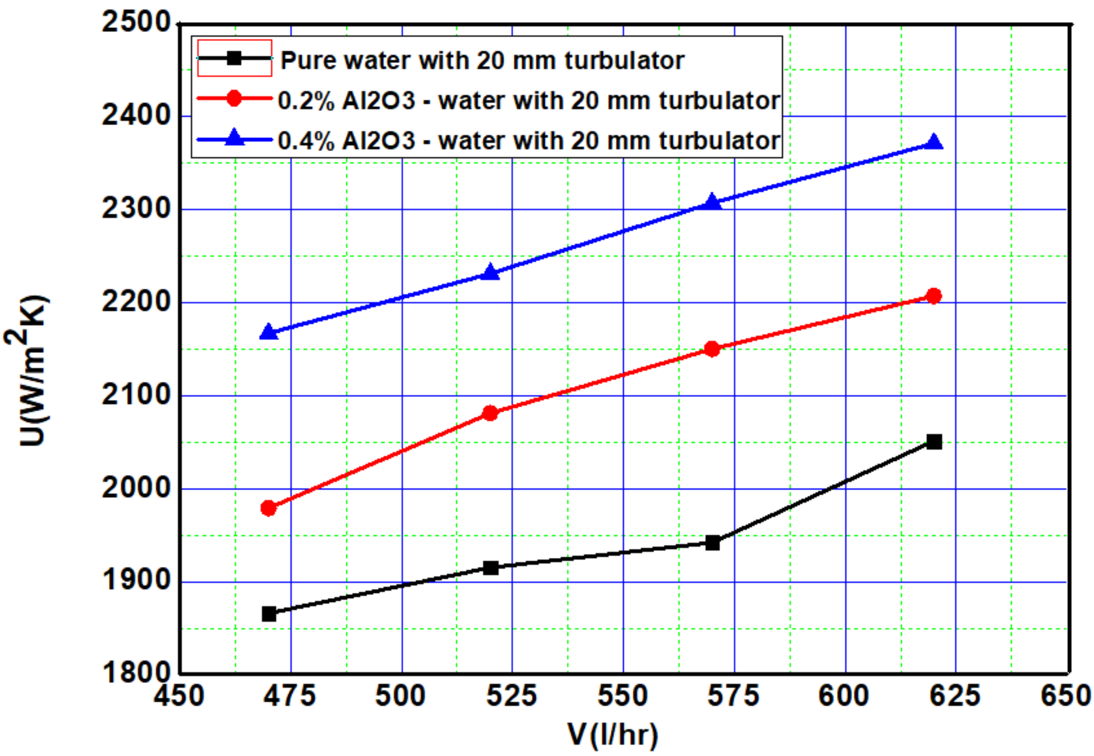

Figure 4.10: Overall heat transfer coefficient vs flow rate for different concentration nanofluid with 20 mm turbulator

4.10 Comparision of Pressure drop with different flow rate for different concentration nanofluid

Figure 4.11 shows the impact of different concentrations of nanofluid on pressure drop. The pressure drop increases by 17.37% to 25% for 0.2 wt% Al_2O_3-water nanofluids and between 30.4% to 50% for 0.4 wt% nanofluids at certain flow rates when compare with pure water. This increase is attributed to higher viscosity and density of nanofluids due to nanoparticle addition, resulting in increased frictional forces and consequently greater pressure drop, as discussed in previous studies (Shabi et al., 2024).

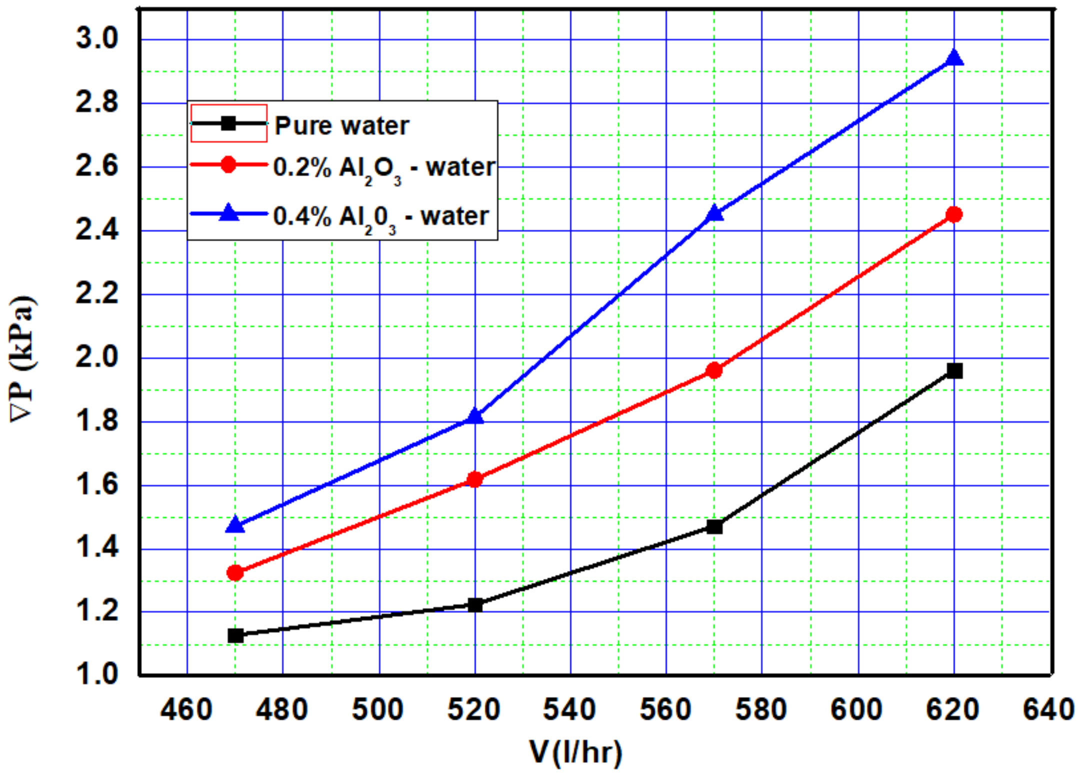

Figure 4.11: Pressure drop vs Flow rate for different concentration nanofluid

4.11 Comparision of Pressure drop with different flow rate for different turbulator for pure water

Figure 4.12 shows the impact of using turbulators on pressure drop in pure water. Compared to experiments conducted solely with water, significant increases in pressure drop are observed when helical coil turbulators are employed. Specifically, compared to the pressure drop observed with pure water, the addition of a 16mm helical coil turbulator increased pressure drop by 768% to 1651%, while the addition of a 20mm helical coil turbulator increased pressure drop by 760% to 1025% at specific flow rates. This substantial increase is attributed to the heightened turbulence and increased flow resistance caused by the helical coil turbulators, which disrupt the flow, leading to greater frictional forces and consequently higher pressure drop, as discussed in previous studies (Ayurek et al., 2018).

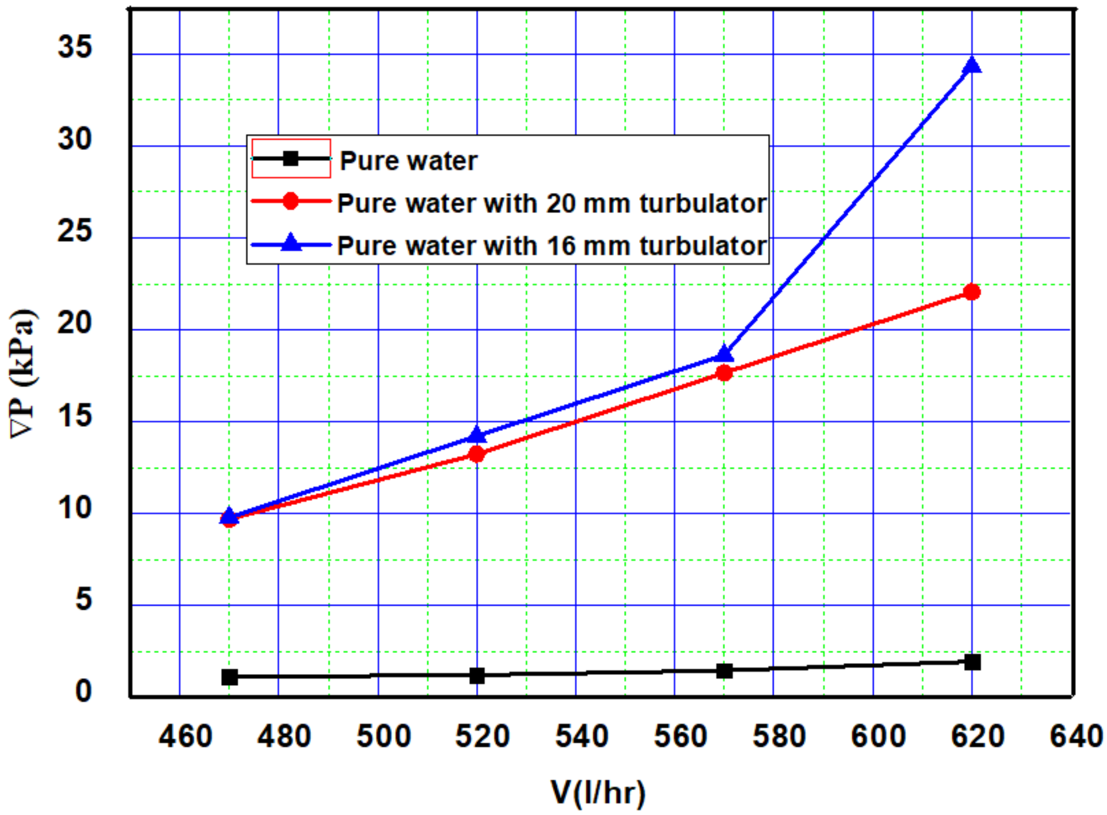

Figure 4.12: Pressure drop vs Flow rate for different turbulator for pure water

4.12 Comparision of Pressure drop with different flow rate for 0.2% nanofluid with different turbulator

Figure 4.13 shows that the pressure drop is minimum for 0.2% nanofluid without turbulator. When turbulators are used in conjunction with nanofluids, the resulting pressure drop values closely approximate those observed with pure water and turbulators. For instance, compared to the pressure drop recorded with 0.2% nanofluid, the addition of 16mm helical coil turbulator in the nanofluid increased pressure drop by 714% to 1500%, while addition of 20mm helical coil turbulator increased pressure drop by 633% to 920% at specific flow rates.

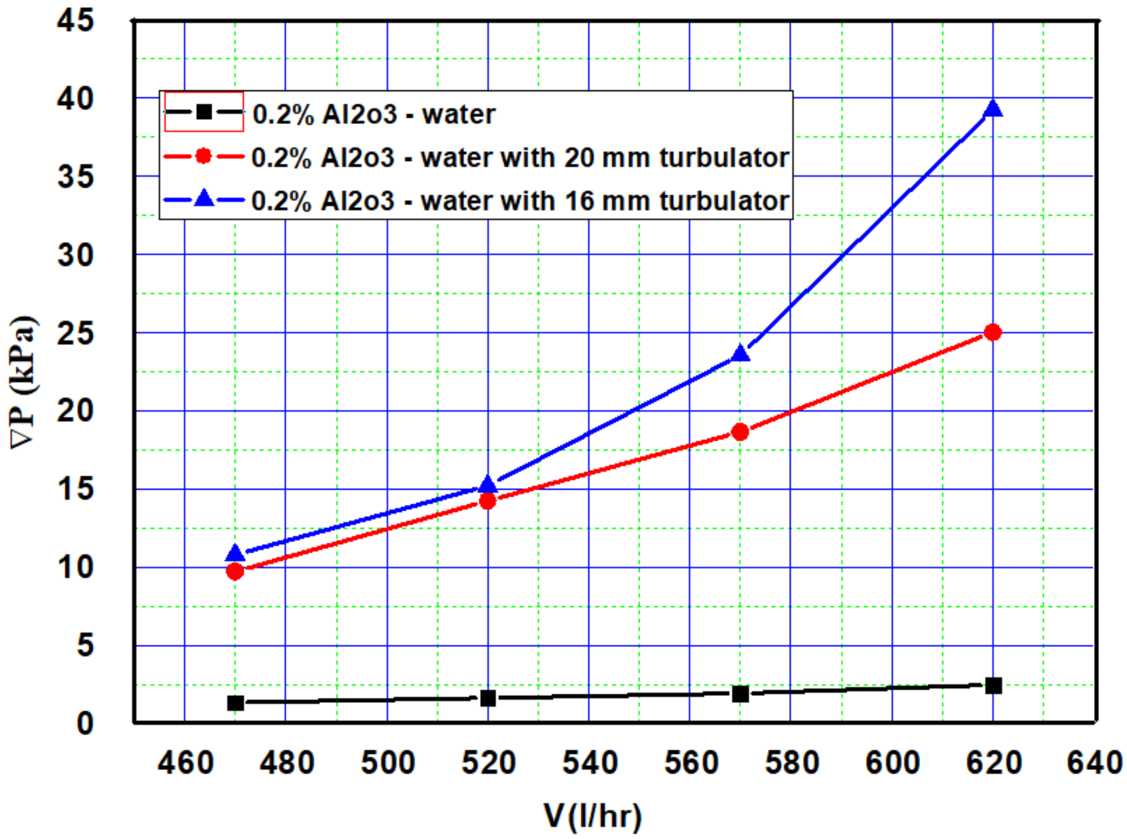

Figure 4.13: Pressure drop vs Flow rate for 0.2% nanofluid with different turbulator

4.13 Comparision of Pressure drop with different flow rate for 0.4% nanofluid with different turbulator

Figure 4.14 shows that the pressure drop is minimum for 0.4% nanofluid without turbulator. When turbulators are utilized alongside nanofluids, the pressure drop values closely resemble those observed with pure water and turbulators. For instance, compared to the pressure drop recorded with 0.4% nanofluid, addition of 16mm helical coil turbulator in pure water increased pressure drop by 693% to 1266%, while addition of a 20mm helical coil turbulator increased pressure drop by 626% to 816% at specific flow rates.

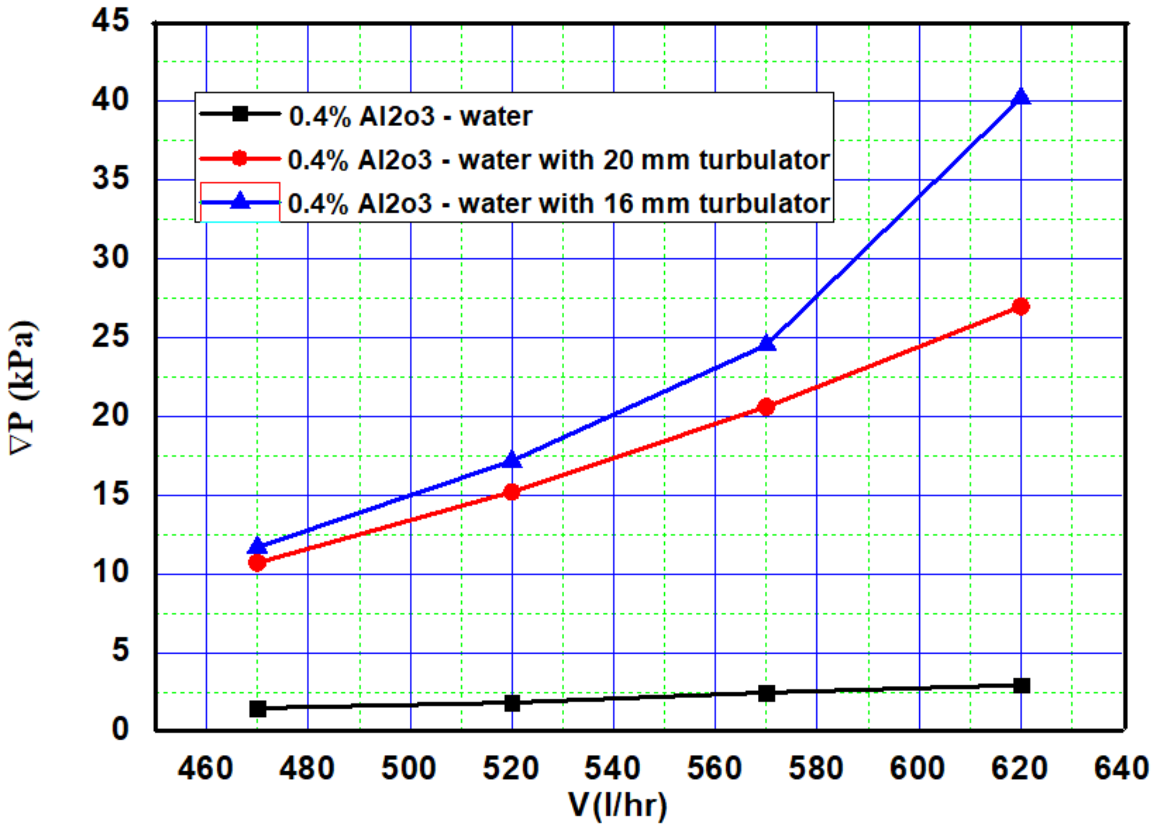

Figure 4.14: Pressure drop vs Flow rate for 0.4% nanofluid with different turbulator

4.14 Comparision of Pressure drop with different flow rate for different concentration nanofluid for 16 mm turbulator

Fig. 4.15 shows increases in pressure drop for 0.2% and 0.4% Al2O3-water nanofluids with 16 mm turbulator compare to pure water used with a 16 mm turbulator. The pressure drop increases for 0.2% and 0.4% Al2O3-water nanofluids range between 10% and 14.29%, and between 17.14% and 19%, respectively, compare to pure water with a 16 mm turbulator at specific flow rates.

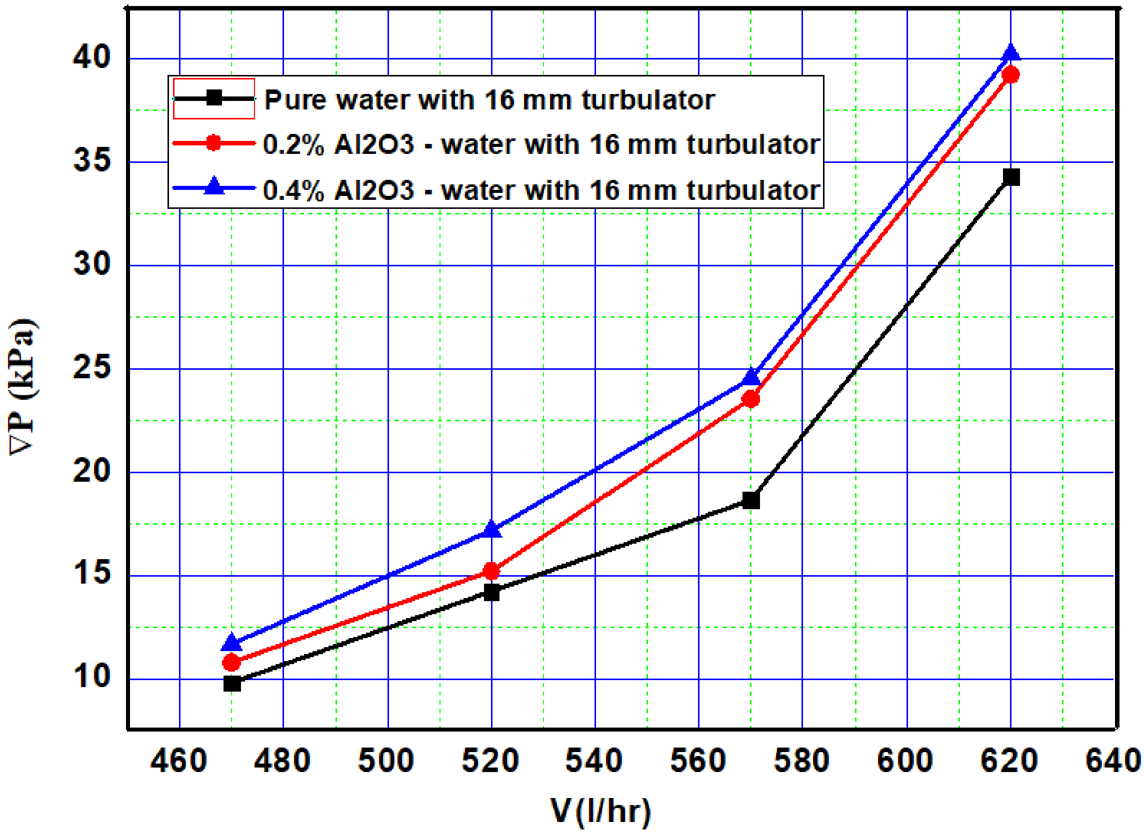

Figure 4.15: Pressure drop vs Flow rate for different concentration with 16 mm turbulator

4.15 Comparision of Pressure drop with different flow rate for different concentration nanofluid for 20 mm turbulator

Fig. 4.16 illustrates the increases in pressure drop with addition of a 20mm helical coil turbulator into 0.2% and 0.4% Al_2O_3-water nanofluids compare with pure water used with a 20mm helical coil turbulator. At specific flow rate values, the pressure drop increases for 0.2% and 0.4% Al_2O_3-water nanofluids range between 1.03% and 13.33%, and between 10.1% and 22.22%, respectively, compared with pure water with a 20mm helical coil turbulator.

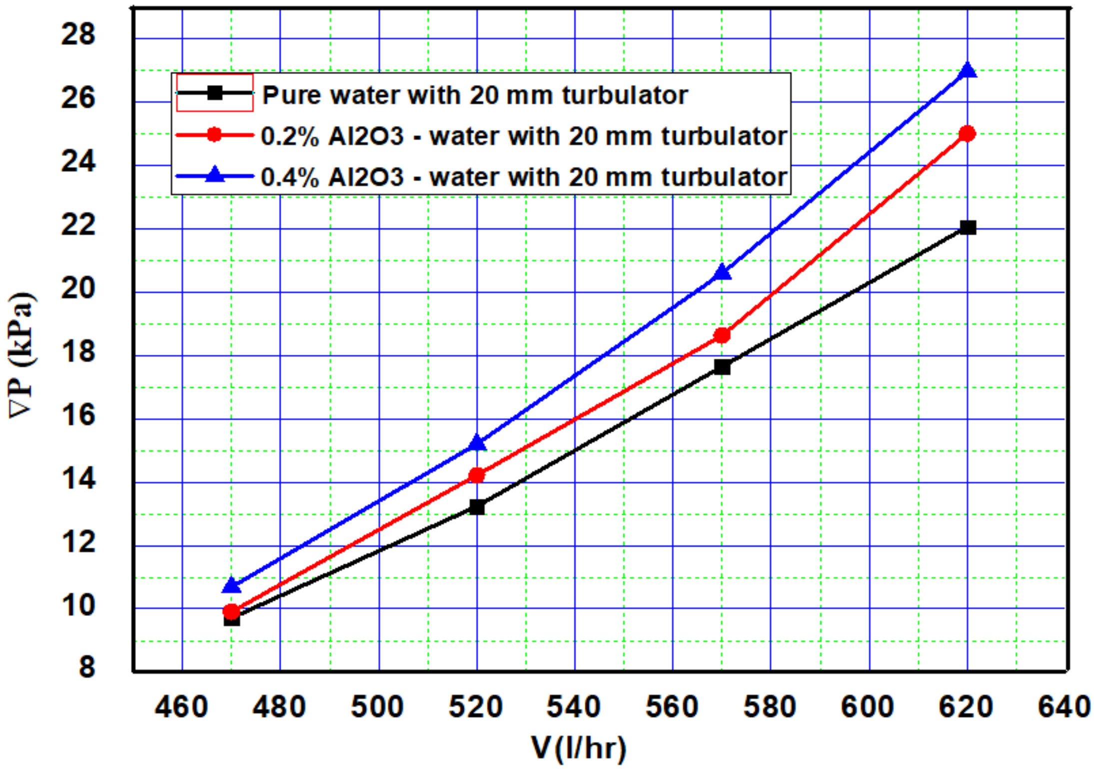

Figure 4.16: Pressure drop vs flow rate for different concentration nanofluid with 20 mm turbulator

4.16 Comparision of Experimental and Numerical of Heat transfer Coeffiecient for different flow rate for pure water and 0.2% concentration of nanofluid

Overall heat transfer coefficient value obtained at different flow rate for Numerical is slightly greater than experimental value. The fig. 4.17 and 4.18 shows overall heat transfer coefficient at different flow rate for numerical and experimental value. Experimental value obtained for heat transfer coefficient of pure water at different flow rate 470 , 520 ,570 and 620 l/hr are 15.79% , 15.68% , 15.02% and 13.46% respectively, lesser than numerical value and for 0.2% concentration of Al2O3 nanofluid at different flow rate 470 , 520 ,570 and 620 l/hr are 11.09% , 8.1% , 4.95% and 3.6% respectively, lesser than numerical value. Both exhibit a similar trend with minor variations between them. These variations could be attributed to the CFD tool's omission of natural attenuation in simulations. Additionally, discrepancies may arise from the properties considered by the CFD tool during simulation compared to actual physical conditions.

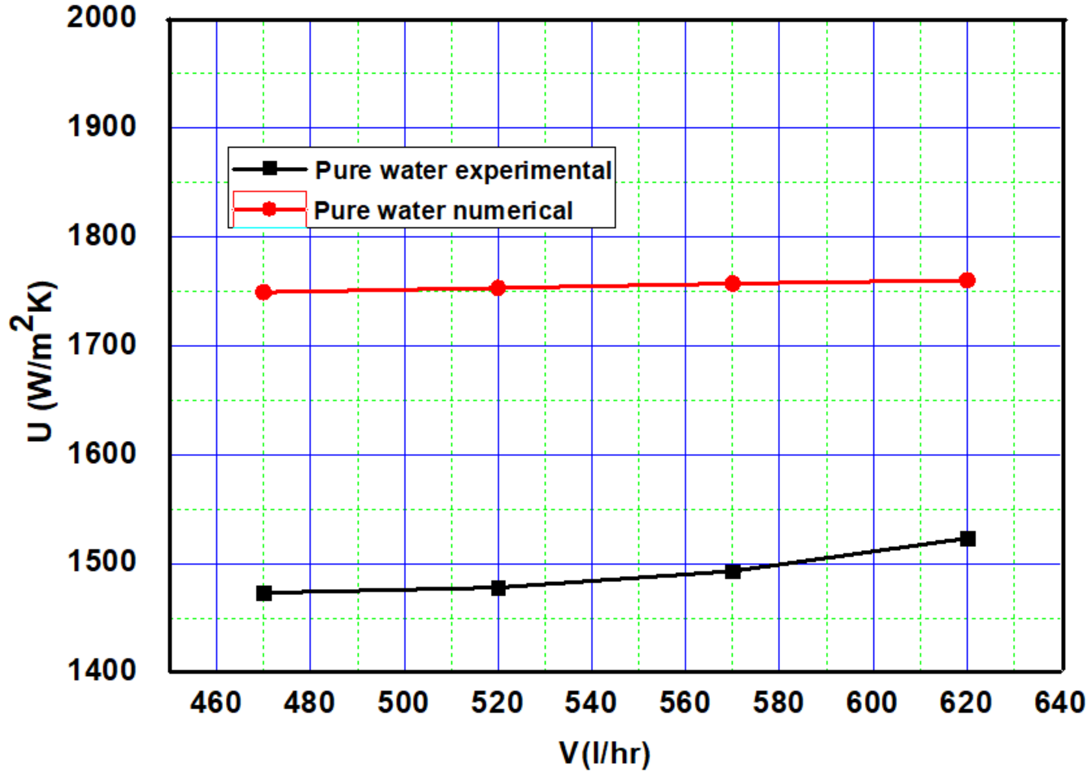

Figure 4.17: Overall Heat Transfer Coefficient vs flow rate for pure water

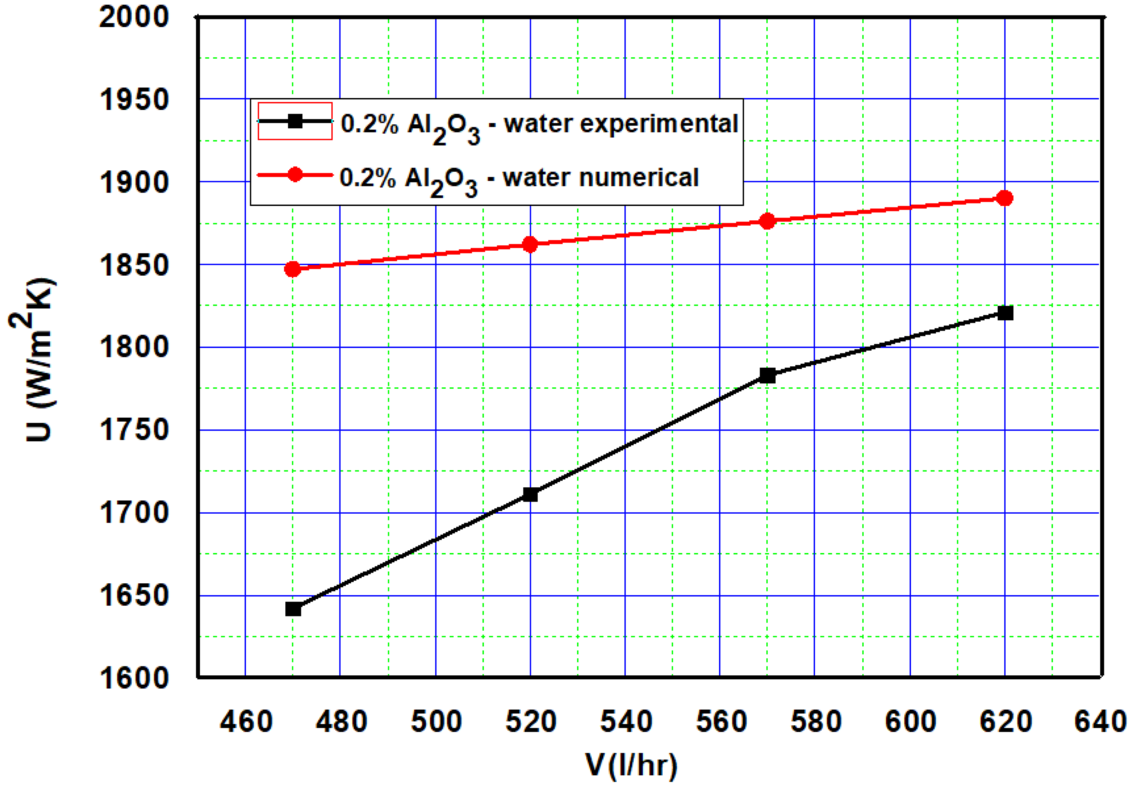

Figure 4.18: Overall Heat Transfer Coefficient vs flow rate for 0.2% concentration nanofluid

4.17 Comparision of Experimental and Numerical of Pressure drop for different flow rate for pure water and 0.2% concentration of nanofluid

The pressure drop value obtained at different flow rate for Numerical is slightly greater than experimental value. The figure 4.19 and 4.20 shows the pressure drop at different flow rate for numerical and experimental value. The experimental value of pressure drop for pure water at different flow rate 470 , 520 ,570 and 620 l/hr are 18.32, 24.89 , 22.4 and 9.92% respectively, lesser than numerical value. The experimental value of pressure drop for 0.2% concentration of Al2O3 nanofluid at different flow rate 470 , 520 ,570 and 620 l/hr are 24.13 , 21.07 , 17.5 and 10.12% respectively, lesser than numerical value. Both exhibit a similar trend with minor variations between them.

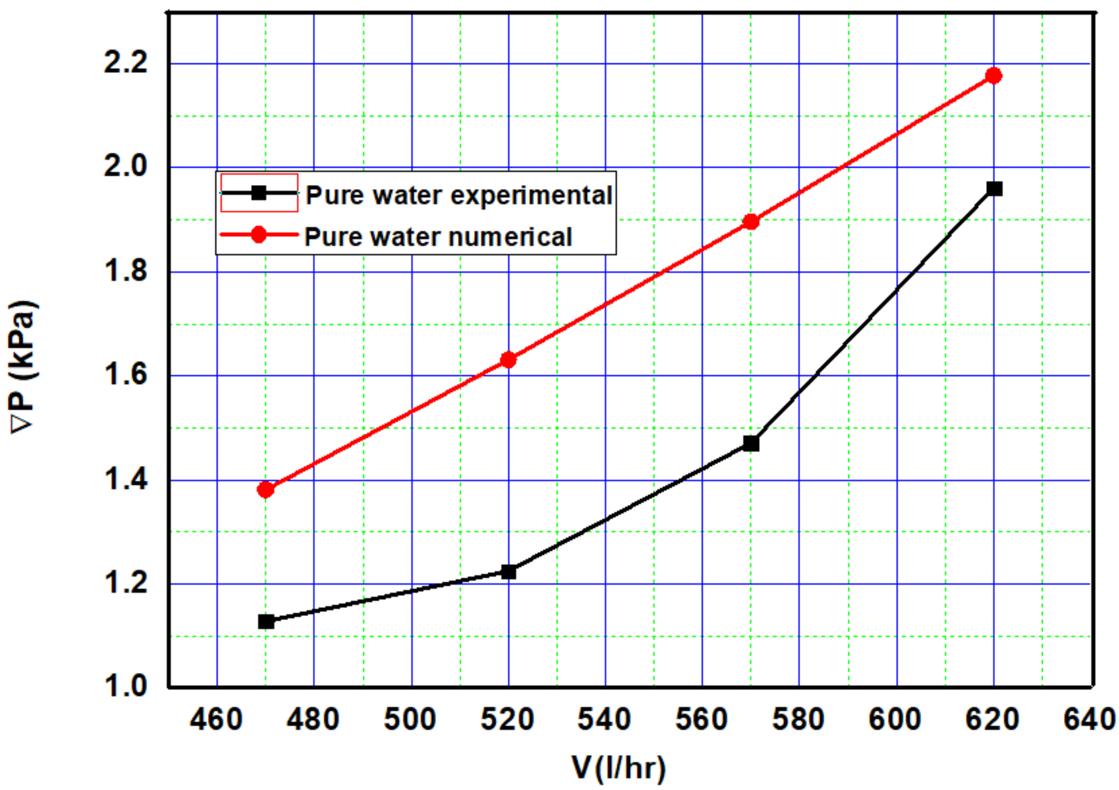

Figure 4.19: Pressure drop vs flow rate for pure water

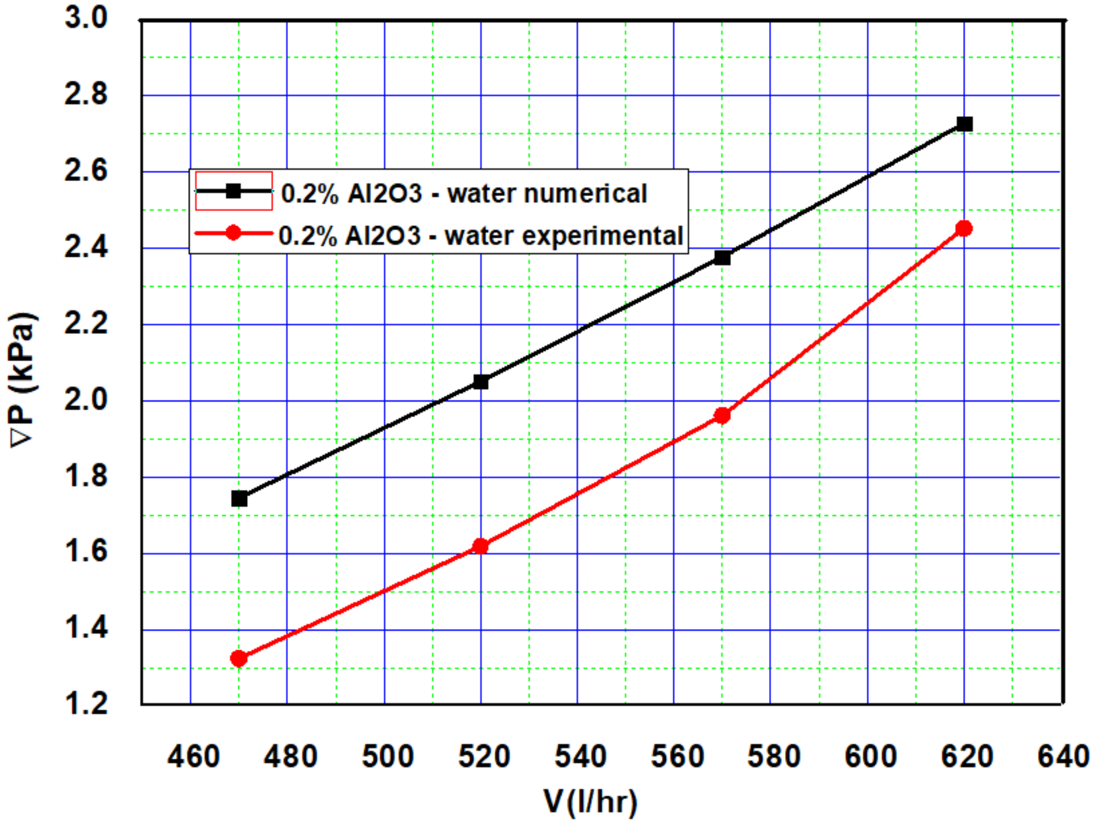

Figure 4.20: Pressure drop vs flow rate for 0.2% concentration nanofluid

CHAPTER FIVE: CONCLUSIONS AND RECOMENDATIONS

5.1 Conclusions

This research investigates the impact of Al_2O_3-water nanofluids and helical coil turbulators on overall heat transfer coefficient and pressure drop in shell and tube heat exchanger. The study explores nanofluid concentrations of 0.2% and 0.4%, along with helical coil turbulators of 16mm and 20mm pitches, aiming to optimize heat exchanger performance.

Experimental findings reveal significant enhancements in convective heat transfer coefficient and thermal conductivity due to inclusion of Al_2O_3 nanoparticles in pure water. Specifically, Al_2O_3-water nanofluids demonstrate marked improvements in heat transfer efficiency compared with pure water. Additionally, use of helical coil turbulators intensifies these enhancements by inducing turbulence, thereby increases the overall heat transfer coefficient.

However, the study identifies a trade-off between improved heat transfer and increased pressure drop. Higher nanoparticle concentrations and tighter pitch turbulators result in substantial pressure drops, potentially leading to higher pumping costs. This underscores the importance of optimizing these parameters to balance improved heat transfer against increased operational costs.

Furthermore, comparative analyses with pure water and nanofluids without turbulators confirm that combining nanofluids and turbulators yields superior thermal performance.

Overall heat transfer coefficient of pure water increases by 3.4% between flow rates of 470 and 620 l/hr. The addition of 0.2% and 0.4% Al_2O_3-water nanofluids without turbulators increases overall heat transfer coefficient by 11.47% to 19.5% and 20.77% to 34.66%, respectively, compare with pure water. Introducing 16mm and 20mm helical coil turbulators in pure water, increases overall heat transfer coefficient by 47.09% to 54.76% and 26.7% to 34.66%, respectively, compare with pure water.

With addition of a 16mm helical coil turbulator, overall heat transfer coefficient increases from 58.92% to 67% for 0.2% and 82.95% to 93.95% for 0.4% Al_2O_3-water nanofluids, flow rates from 470 to 620 l/hr, compare with pure water without turbulators.

Pressure drop of pure water increases by 73.84% between flow rates of 470 and 620 l/hr. For 0.2% and 0.4% Al_2O_3-water nanofluids, the pressure drop increases by 17.37% to

25% and 30.4% to 50%, respectively, compared to pure water without turbulators. Introducing 16mm and 20mm pitch helical coil in pure water increases pressure drop by 768% to 1651% and 760% to 1025%, respectively, at the specific flow rate.

The pressure drop for 0.2% and 0.4% Al_2O_3-water nanofluids with 16mm turbulators increases by 855.4% to 1900% and 934.57% to 1950%, respectively, at flow rates ranging from 470 to 620 l/hr compared to pure water without turbulators.

5.2 Recommendations

The recommendations which are proposed for further exploration in this field are as follows:

- Investigate the effect of varying nanoparticle concentrations on both heat pressure drop and heat transfer efficiency.
- Explore diverse types of nanoparticles for optimize the performance of nanofluids.
- Examine hybrid nanofluids containing multiple types of nanoparticles to enhance thermal properties.
- Investigate different geometries and configurations of turbulated tubes to identify optimal designs.
- Optimize insert geometries to enhance heat transfer rates while managing pressure drop effectively.
- Assess the practical benefits and challenges of integrating Al_2O_3 nanofluids and turbulated tubes in industrial applications.
- Explore the influence of different base fluids (e.g., oils, ethylene glycol,water) on the performance of Al_2O_3 nanofluids.
- Conduct comparative studies on fluid flow and heat transfer characteristics using various base fluids.

REFERENCES

- Arun Kumar Tiwari, Pradyumna Ghosh and Jahar Sarkar, Particle concentration levels of various nanofluids in plate heat exchanger for best performance, International Journal of Heat and Mass Transfer, 2015, 89, 1110-1118.
- Almohammadi, Hamed & Nasirivatan, Shahin & Esmaeilzadeh, Esmaeil & Motezakker, Ahmad & Nokhosteen, Arman., Experimental Investigation of Convective Heat Transfer and Pressure Drop of Al2O3-Water Nanofluid in Laminar Flow Regime inside a Circular Tube. World Academy of Science, Engineering and Technology, 2012, 68, 1187-1192.
- Chandrasekhar, S., Suresh, S., & Venkitaraj, K. P., Experimental investigation on heat transfer and friction factor of water based Al2O3 nanofluid in a horizontal tube under turbulent flow, Experimental Thermal and Fluid Science, 2016, 73, 1-11.
- Eda Feyza Akyürek, Kadir Geliş, Bayram Şahin, Eyüphan Manay, Experimental analysis for heat transfer of nanofluid with wire coil turbulators in a concentric tube heat exchanger, Results in Physics, 2018, 9, 376-389.
- Fluent A., Ansys Fluent Theory Guide. ANSYS Inc., USA, 2017.
- Jaafar Albadr, Satinder Tayal, Mushtaq Alasadi, Heat transfer through heat exchanger using Al2O3 nanofluid at different concentrations, Case Studies in Thermal Engineering, 2013, 1, 38-44.
- Jian Guo, Aiwu Fan, Xiaoyu Zhang and Wei Liu, A Numerical Study on Heat Transfer and Friction Factor Characteristics of Laminar Flow in a Circular Tube Fitted with Center Cleared Twisted Tape, International Journal of Thermal Sciences, 2011, 50(7), 1263-1270.
- Joseph Owolabi and Pius Ojadi, "Synthesis, characterization and x-ray diffraction analysis of aluminum oxide nanomaterials". FUW Trends in Science & Technology Journal, 2023, 8(3), 423-427.
- Hussein, Adnan, Experimental measurement of nanofluids thermal properties. International Journal of Automotive and Mechanical Engineering, 2013, 7, 2229-8649.
- K. Kamboj, G. Singh, Sharma, R. Sharma. Heat transfer augmentation in double pipe heat exchanger using mechanical turbulators, Heat and Mass Transfer, 2017, 53, 553-567.

- Kevin Apmann, Ryan Fulmer, Alberto Soto, and Saeid Vafaei, Thermal Conductivity and Viscosity: Review and Optimization of Effects of Nanoparticles, Materials, 2021, 14(5), 1291.
- Mohammad Fares, Mohammad AL-Mayyahi, Mohammed AL-Saad, Heat transfer analysis of a shell and tube heat exchanger operated with graphene nanofluids, Case Studies in Thermal Engineering, 2020, 18, 100584.
- M. Pimsarn, P. Samruaisin, P. Eiamsa-ard, N. Koolnapadol, P. Promthaisong, S. Eiamsa-ard, Enhanced forced convection heat transfer of a heat exchanger tube utilizing serrated-ring turbulators, Case Studies in Thermal Engineering, 2021, 28, 101570.
- Murugesan, P., Sivanandham, V., Suresh, S., & Venkatachalapathy, K., Experimental investigation on heat transfer and friction factor characteristics of CuO-water nanofluid in a circular tube with twisted tape inserts, Experimental Thermal and Fluid Science, 2017, 86, 102-112.
- Omar Ali Shabi, Majed Alhezmy, El-Sayed R. Negeed, Khaled O.Elzoghaly, Experimental investigation of shell and helical coiled heat exchanger with Al2O3 nanofluid with wide range of particle concentration, Frontiers in Mechanical Engineering, 2024, 10.
- Ramesh K. Shah and Dusan P. Sekulic, Fundamentals of Heat Exchanger Design, John Wiley and Sons Inc., 2003.
- Rohit S. Khedkar, Shriram S. Sonawane, Kailas L., Wasewar, Influence of CuO nanoparticles in enhancing the thermal conductivity of water and monoethylene glycol based nanofluids, International Communications in Heat and Mass Transfer, 2012, 39(5), 665-669.
- Sarit Das, Stephen Choi, Hrishikesh Patel, Heat transfer in nanofluid – a review, Heat Transfer Engineering, 2006, 27(10), 3-19.
- Seyedmahmood Kia, Shoaib Khanmohammadi, Ali Jahangiri, Experimental and numerical investigation on heat transfer and pressure drop of SiO2 and Al2O3 oil-based nanofluid characteristics through the different helical tubes under constant heat fluxes, International Journal of Thermal Sciences, 2023, 185, 108082.
- Shahrul, I.M. Sharul & Islam, Mohammed Mahbubul & Rahman, Saidur & Shah, Sheikh Khaleduzzaman & Mohd Sabri, Mohd Faizul & Rahman, M., Effectiveness

Study of a Shell and Tube Heat Exchanger Operated with Nanofluids at Different Mass Flow Rates, Numerical Heat Transfer Applications, 2014, 65(7), 699-713.

- S. Lee, S.U.S. Choi, S. Li, J.A. Eastman, Measuring thermal conductivity of fluids containing oxide nanoparticles, Journal of Heat Transfer, 1999, 121, 280-289.
- Sowmya Tippa, Marneni Narahari and Rajashekhar Pendyala, Unsteady natural convection flow of nanofluids past a semi-infinite isothermal vertical plate, AIP Conference Proceedings, 2016, 1787, 020014.
- Suresh S, Selvakumar P, Chandrasekar M, Srinivasa Raman V. Experimental studies on heat transfer and friction factor characteristics of Al2O3/water nanofluid under turbulent flow with spiraled rod inserts. Chemical Engineering Process, 2012, 53, 24-30.
- Tareq Salameh, Malek Alkasrawi, Abdul Ghani Olabi, Ahmed Al Makky, Mohammad Ali Abdelkareem, Experimental and numerical analysis of heat transfer enhancement inside concentric counter flow tube heat exchanger using different nanofluids. International Journal of Thermofluids, 2023, 20, 100432.
- Y. Xuan and Q. Li, Investigation on convective heat transfer and flow features of nanofluids. Journal of Heat Transfer, 2003, 125(1), 151-155.

APPENDIX NO. 1 : EXPERIMENTAL SETUP

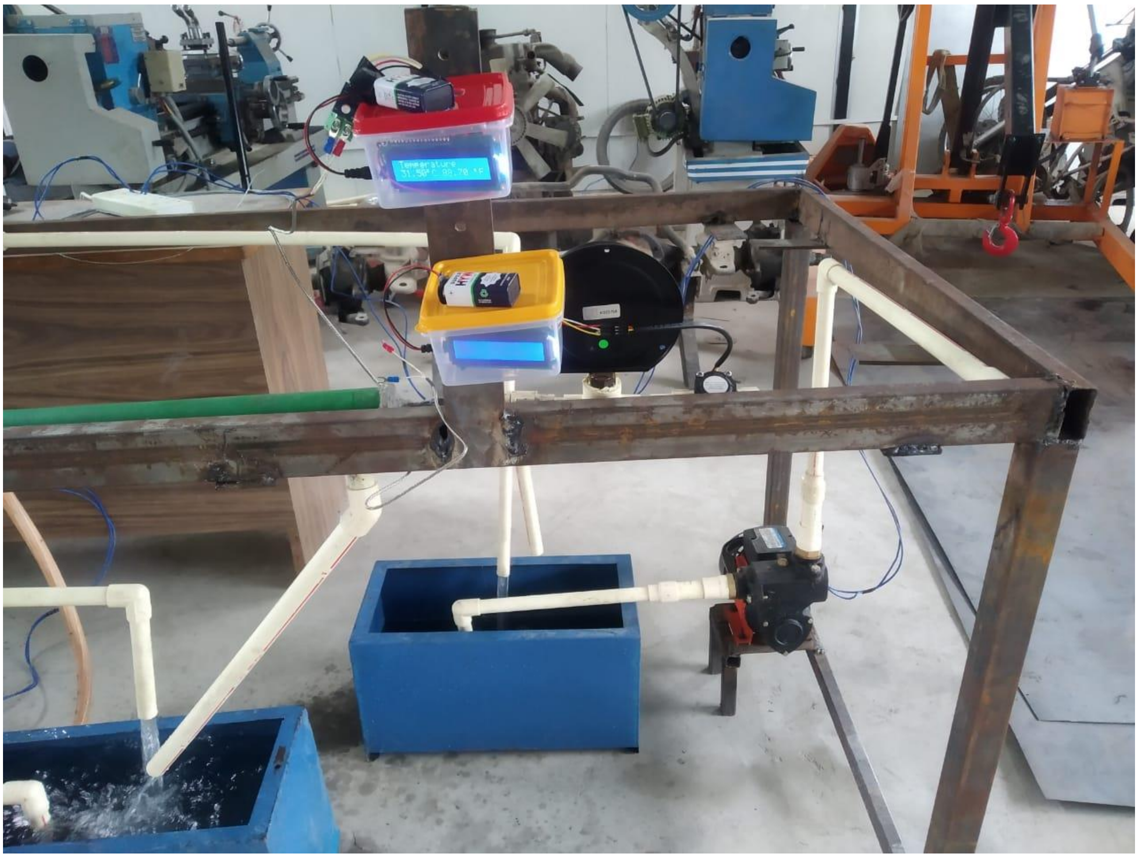

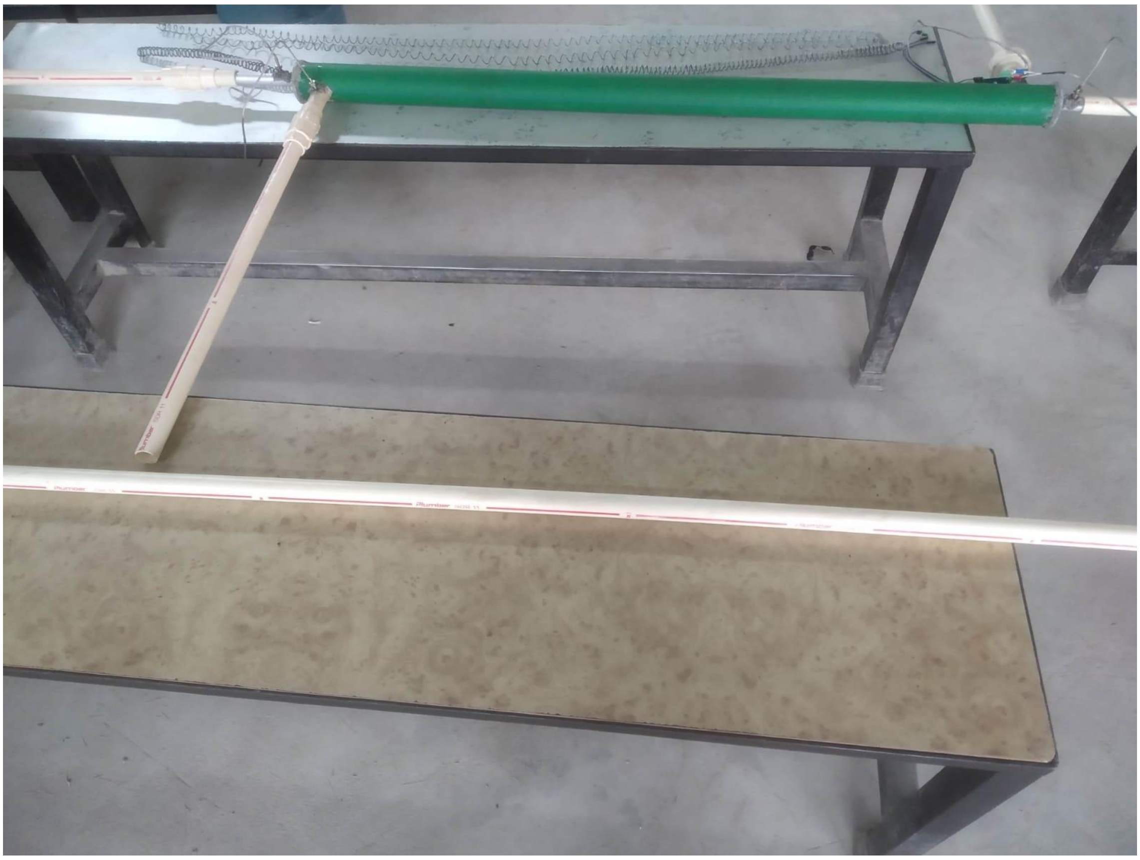

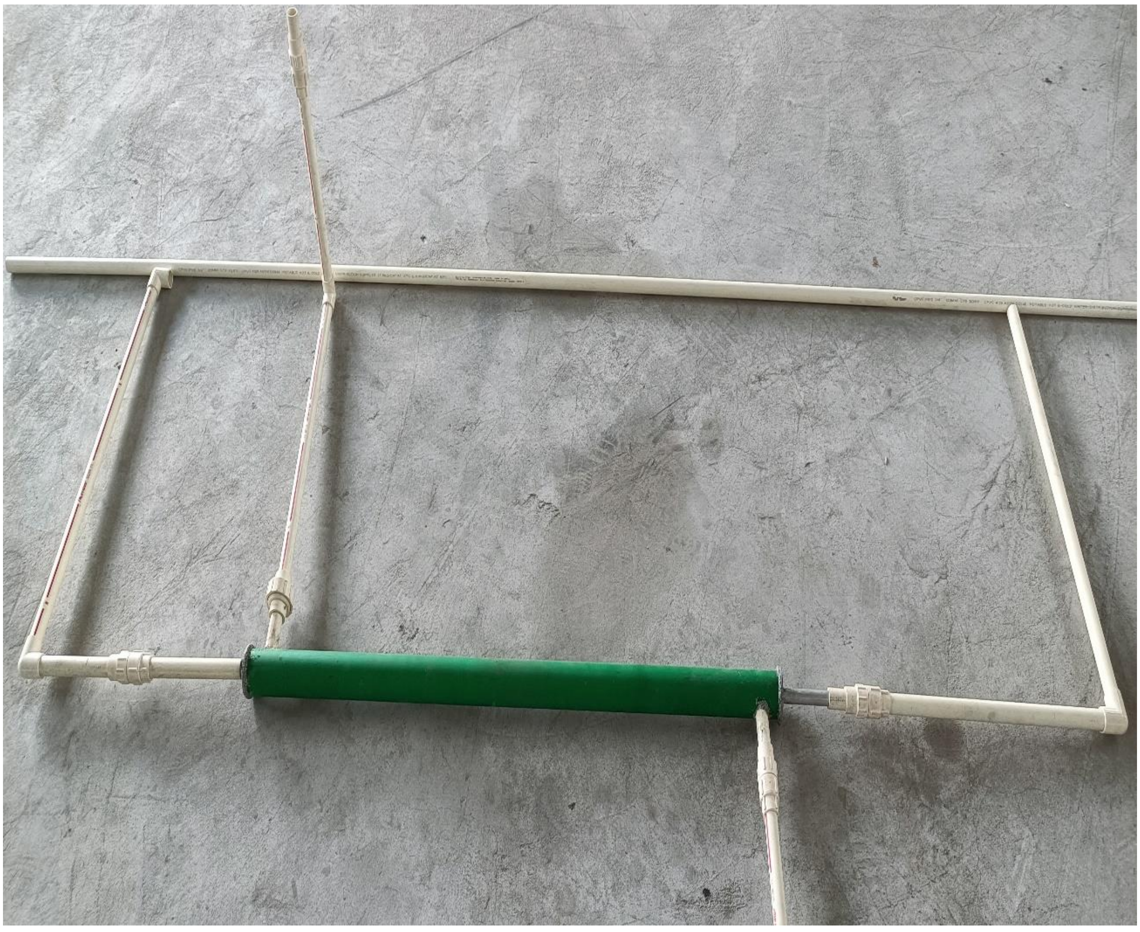

APPENDIX NO. 2: DURING NANOFLUID PREPARATION


METTLER TOLEDO
Net
2.0015 g


Wisd

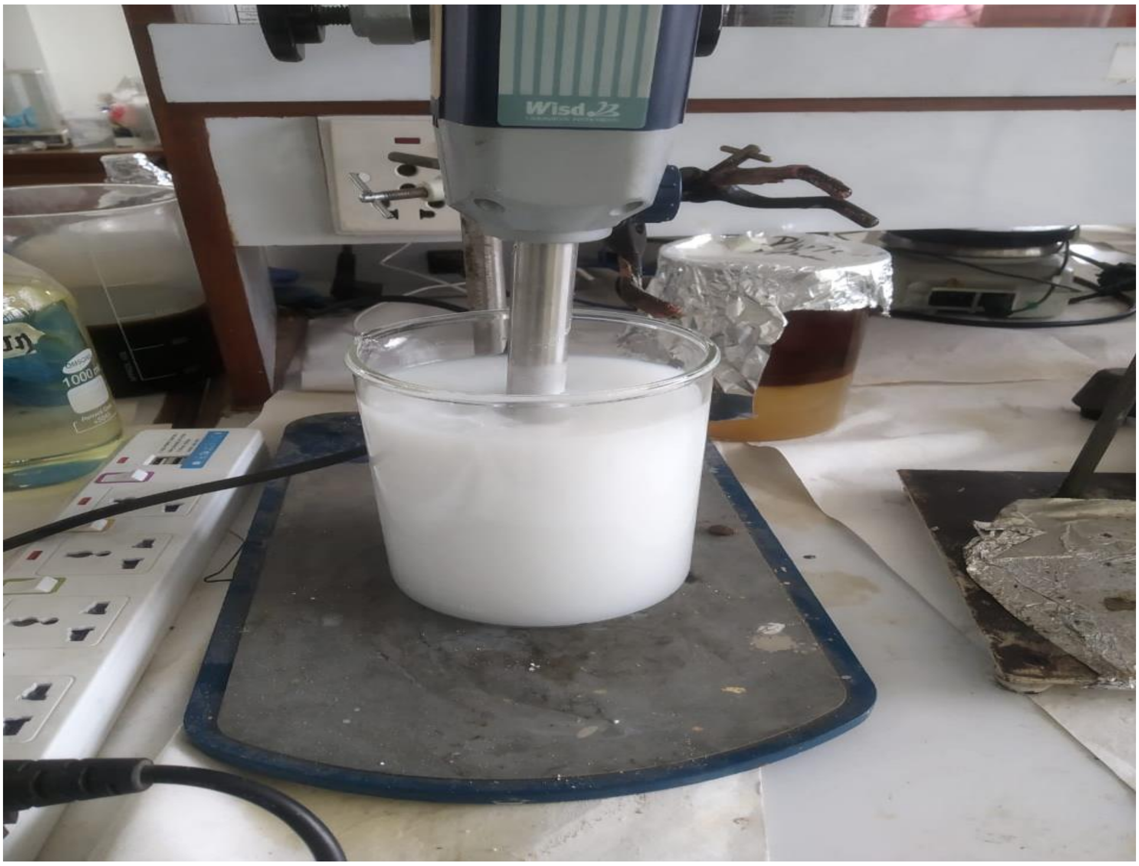
Wisd


POWERSONIC
603
40
POWER
MODE
UP
DOWN
HEAT
START/STOP

APPENDIX NO. 3: OBSERVED DURING EXPERIMENT

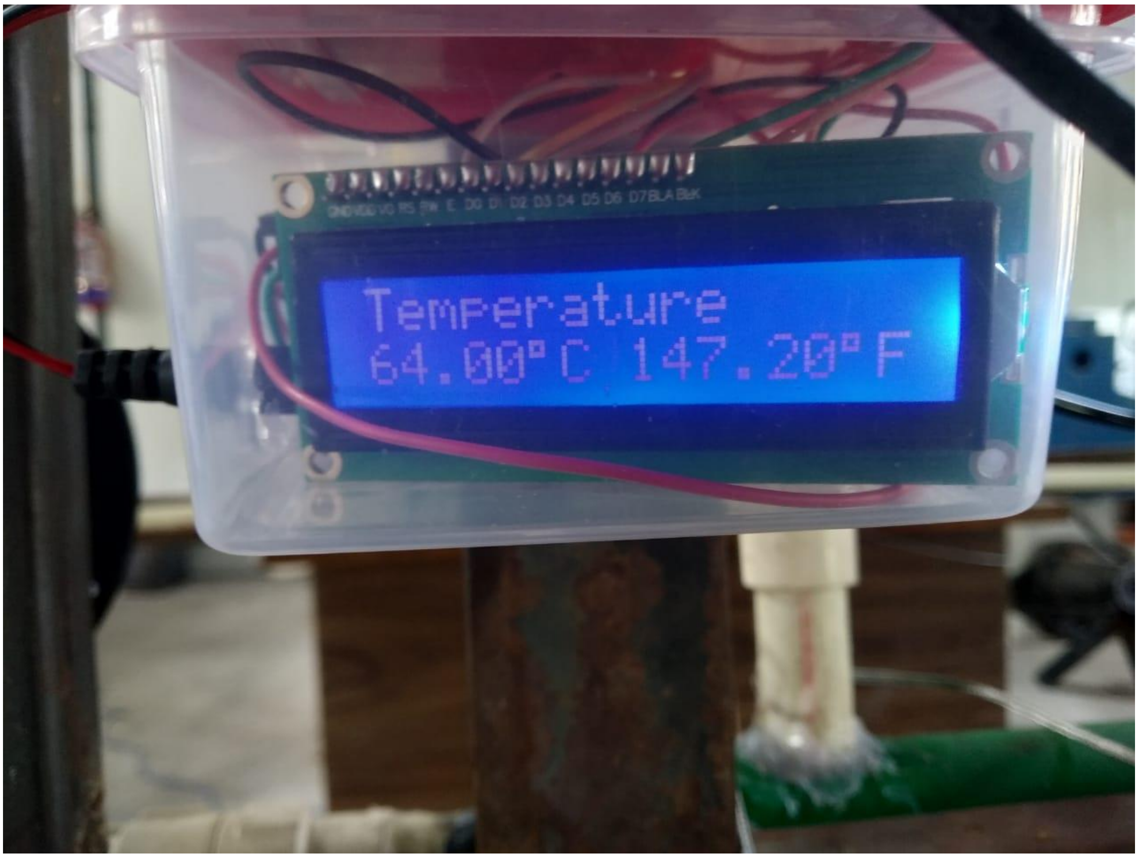
Temperature
64.00°C 147.20°F

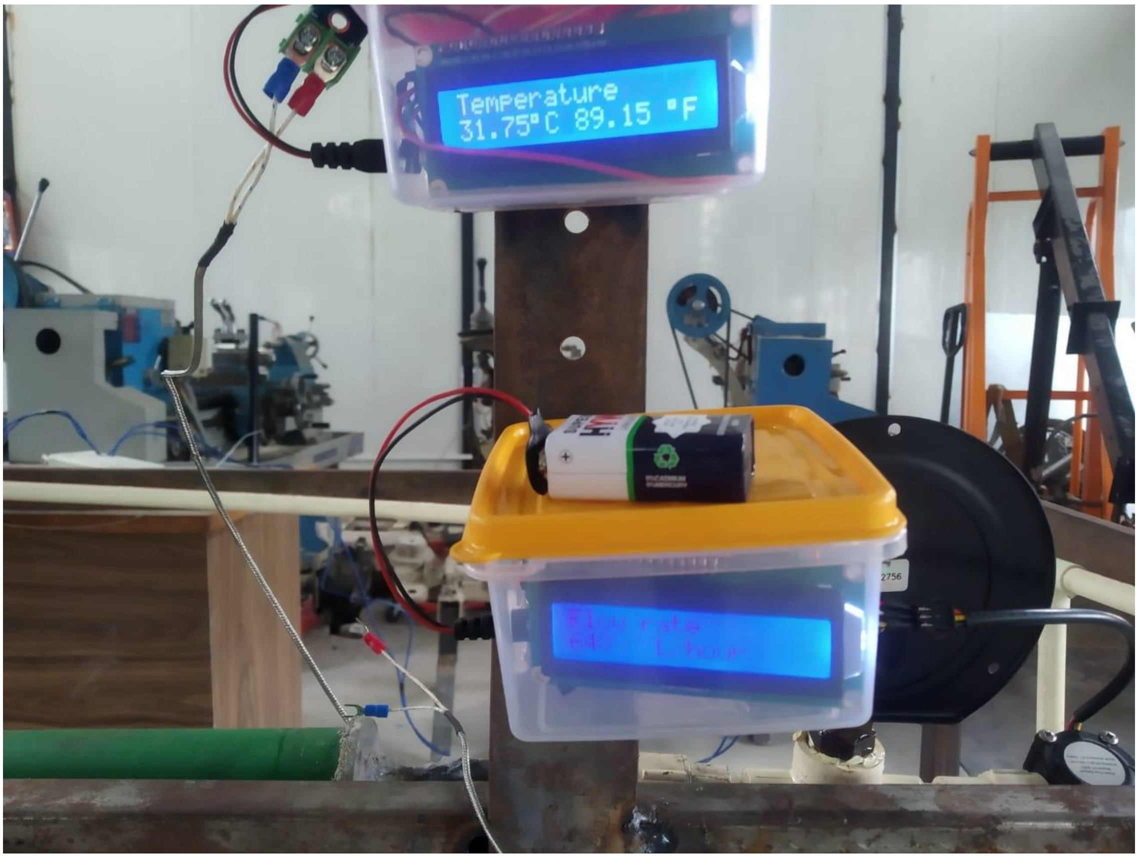
Temperature
31.75°C 89.15 °F

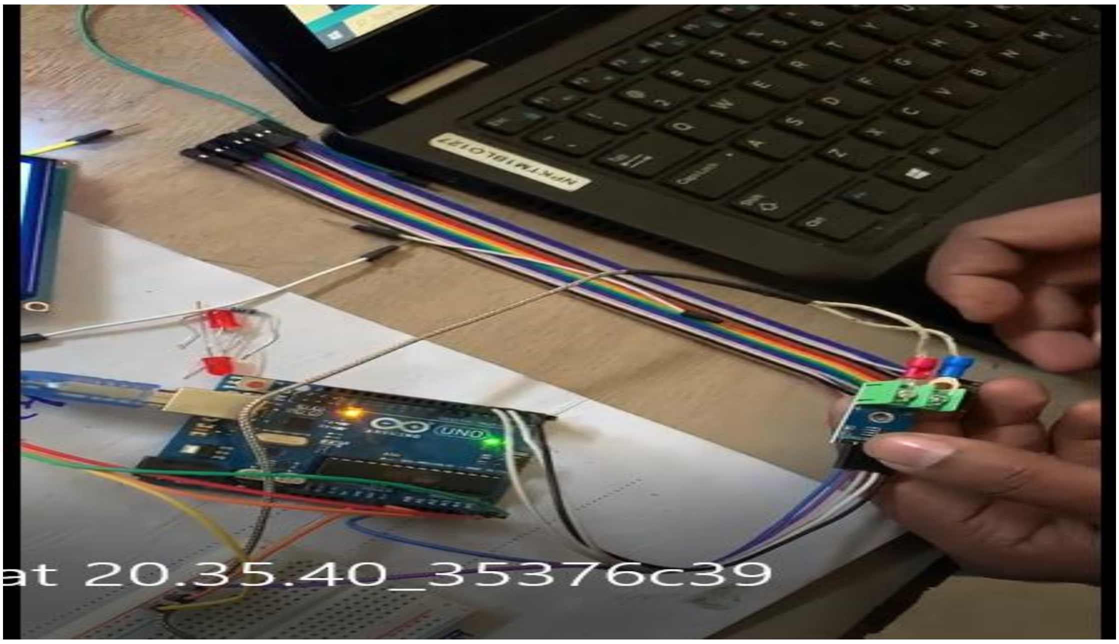
at 20.35.40_35376c39


at 20.35.40_35376c39

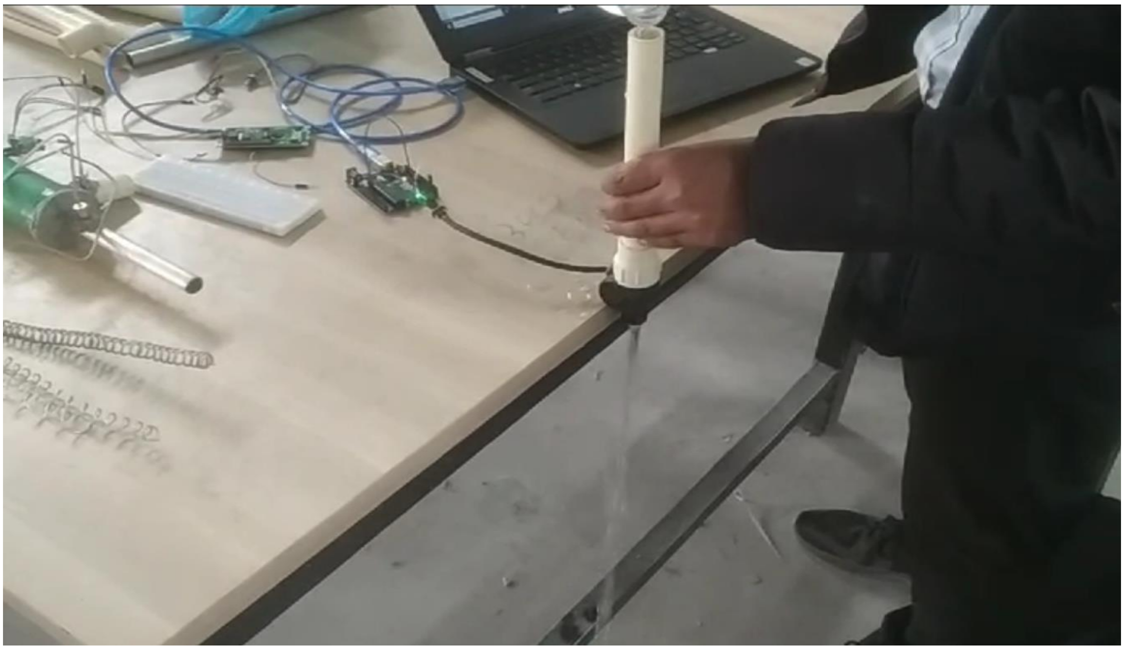

APPENDIX NO. 4: EXPERIMENTAL DATA

S.N.	V_h (l/hr)	V_c (l/hr)	T_{h1} (˚C)	T_{h2} (˚C)	T_{c1} (˚C)	T_{c2} (˚C)	U_o (W/m^2K)	ΔP (kPa)
1	132	470	68	53	26	30	1473	1.128
2	132	520	68	52.5	26	29.5	1478	1.225
3	132	570	68	52.25	26	29.2	1493	1.471
4	132	620	68	52	26	29	1523	1.961

Table : Experimental data of Pure Water without turbulator

S.N.	V_h (l/hr)	V_c (l/hr)	T_{h1} (˚C)	T_{h2} (˚C)	T_{c1} (˚C)	T_{c2} (˚C)	U_o (W/m^2K)	ΔP (kPa)
1	132	470	68	48.5	26	31.4	2167	9.797
2	132	520	68	48	26	31	2231	14.219
3	132	570	68	47.5	26	30.7	2307	18.632
4	132	620	68	47	26	30	2357	34.323

Table : Experimental data of Pure Water with 16mm turbulator

S.N.	V_h (l/hr)	V_c (l/hr)	T_{h1} (˚C)	T_{h2} (˚C)	T_{c1} (˚C)	T_{c2} (˚C)	U_o (W/m^2K)	ΔP (kPa)
1	132	470	68	50.5	26	30.9	1866	9.708
2	132	520	68	50	26	30.5	1915	13.238
3	132	570	68	49.5	26	30.2	1942	17.651
4	132	620	68	49	26	30	2051	22.064

Table : Experimental data of Pure Water with 20mm turbulator

S.N.	V_h (l/hr)	V_c (l/hr)	T_{h1} (˚C)	T_{h2} (˚C)	T_{c1} (˚C)	T_{c2} (˚C)	U_o (W/m^2K)	ΔP (kPa)
1	132	470	68	51.5	26	29.5	1642	1.324
2	132	520	68	51	26	29.8	1711	1.618
3	132	570	68	50.5	26	30	1783	1.961
4	132	620	68	50	26	30.25	1820	2.451

Table : Experimental data of 0.2% Al2O3-Water without turbulator

S.N.	V_h (l/hr)	V_c (l/hr)	T_{h1} (˚C)	T_{h2} (˚C)	T_{c1} (˚C)	T_{c2} (˚C)	U_o (W/m^2K)	ΔP (kPa)
1	132	470	68	47.5	26	31.7	2341	10.777
2	132	520	68	47	26	31.2	2388	15.200
3	132	570	68	46.5	26	30.9	2472	23.535
4	132	620	68	46	26	30.6	2544	39.226

Table : Experimental data of 0.2% Al2O3-water with 16mm turbulator

S.N.	V_h (l/hr)	V_c (l/hr)	T_{h1} (˚C)	T_{h2} (˚C)	T_{c1} (˚C)	T_{c2} (˚C)	U_o (W/m^2K)	ΔP (kPa)
1	132	470	68	49.5	26	31	1979	9.709
2	132	520	68	49	26	30.8	2081	14.219
3	132	570	68	48.5	26	30.5	2150	18.632
4	132	620	68	48	26	30.2	2207	25.006

Table : Experimental data of 0.2% Al2O3-Water with 20mm turbulator

S.N.	V_h (l/hr)	V_c (l/hr)	T_{h1} (˚C)	T_{h2} (˚C)	T_{c1} (˚C)	T_{c2} (˚C)	U_o (W/m^2K)	ΔP (kPa)
1	132	470	68	51	26	30.7	1779	1.471
2	132	520	68	50	26	30.4	1891	1.814
3	132	570	68	49.5	26	30.2	1975	2.451
4	132	620	68	49	26	30	2051	2.941

Table : Experimental data of 0.4% Al2O3-Water without turbulator

S.N.	V_h (l/hr)	V_c (l/hr)	T_{h1} (˚C)	T_{h2} (˚C)	T_{c1} (˚C)	T_{c2} (˚C)	U_o (W/m^2K)	ΔP (kPa)
1	132	470	68	45.5	26	32.2	2695	11.670
2	132	520	68	45	26	31.8	2786	17.161
3	132	570	68	44.5	26	31.4	2862	24.516
4	132	620	68	44	26	31.1	2954	40.207

Table : Experimental data of 0.4% Al2O3-Water with 16mm turbulator

S.N.	V_h (l/hr)	V_c (l/hr)	T_{h1} (˚C)	T_{h2} (˚C)	T_{c1} (˚C)	T_{c2} (˚C)	U_o (W/m^2K)	ΔP (kPa)
1	132	470	68	48.5	26	31.4	2167	10.689
2	132	520	68	48	26	31	2231	15.200
3	132	570	68	47.5	26	30.7	2307	20.593
4	132	620	68	47	26	30.4	2371	16.968

Table : Experimental data of 0.4% Al2O3-Water with 20mm turbulator

APPENDIX NO. 5: NUMERICAL DATA

Vc (l/hr)	Uo (W/m^2K)	ΔP (kPa)
470	1749	1.381
520	1753	1.631
570	1757	1.896
620	1760	2.177

Table : Numerical data of Pure Water without turbulator

Vc (l/hr)	Uo (W/m^2K)	ΔP (kPa)
470	1847	1.745
520	1862	2.050
570	1876	2.377
620	1890	2.727

Table :Numerical data of 0.2% Al2O3-Water without turbulator

APPENDIX NO. 5: PROPERTIES OF DIFFERENT MATERIAL USED

Material	Density	Thermal Conductivity	Specific Heat Capacity
Aluminium	2719	202.4	871
PPR	900	0.21	1700

Table :Properties of different material used

APPENDIX NO. 6: INPUT SOLVER AND SOLUTION PARAMETER USED

<u>Input Solver Parameters in ANSYS FLUENT:</u>

1. Solver:

- Type: Pressure based
- Velocity formulation: Absolute
- Time: Steady condition
- Gravity axis: Y-Direction
- Gravity value taken: -9.81 m/s2
- Energy equation: On
- Viscous model: k-epsilon (2 equation) with Scalable wall functions
- K-epsilon model: Realizable

2. Materials Used:

- Solid Material:
- Polypropylene Random Copolymer (PPR) and Aluminium
- Fluid Material:
- Water and Al2O3-water Nanofluid

3. Boundary condition:

- Hot inlet temperature and velocity: 68 ˚C and 0.18229 m/s^2
- Cold inlet temperature and velocity: 26 ˚C and 0.983 , 1.0878 , 1.1923 and 1.297 m/s^2

<u>Parameters for method and controls of solution of heat exchanger in ANSYS FLUENT</u>:

1. Pressure-velocity coupling: Coupled

2. Spatial Discretization

- Pressure: Second Order
- Momenturm, Energy, Liquid Volume Fraction: Second order upwind

3. Solution Controls:

- All the default value was used.

Experimental Analysis of Fluid Flow and Heat Transfer of Al2O3-Water Nanofluid in Turbulated Tube.docx

ORIGINALITY REPORT

6%

SIMILARITY INDEX

PRIMARY SOURCES

1	elibrary.tucl.edu.np Internet	77 words — 1%
2	Eda Feyza Akyürek, Kadir Geliş, Bayram Şahin, Eyüphan Manay. "Experimental analysis for heat transfer of nanofluid with wire coil turbulators in a concentric tube heat exchanger", Results in Physics, 2018 Crossref	60 words — 1%
3	www.researchgate.net Internet	45 words — < 1%
4	mdpi-res.com Internet	34 words — < 1%
5	repository.ju.edu.et Internet	29 words — < 1%
6	ouci.dntb.gov.ua Internet	27 words — < 1%
7	www.ijsr.net Internet	27 words — < 1%
8	Sharma, P.. "Enhancement of thermal conductivity of ethylene glycol based silver nanofluids", Powder Technology, 20110310	20 words — < 1%

[aet] Editor Decision Inbox ×

postmaster@nepjol.info 11:25 (1 hour ago)

to Surya, me

Surya Adhikari, Sudeep Sah:

We have reached a decision regarding your submission to Advances in Engineering and Technology: An International Journal, **"Experimental Analysis of Fluid Flow and Heat Transfer of Al2o3-Water Nanofluids in Turbulated Tube"**.

Our decision is to: **Accept Submission.**

____

Advances in Engineering and Technology: An International Journal